ARIZONA DEPARTMENT OF TRANSPORTATION

REPORT: ADOT-RS-15(164) FINAL REPORT — PHASE I

TESTING METHODS FOR ASPHALT-RUBBER

Prepared by:
Dr. R.A. Jimenez, C.E. Dept.
Arizona Transportation & Traffic Institute
College of Engineering
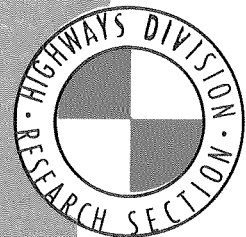The University of Arizona
Tucson, Arizona 85721

January 1978

35-049

Final Report - Phase I

TESTING METHODS FOR ASPHALT-RUBBER

by

R. A. Jimenez

Report Number ATTI-78-1

Submitted to

The Arizona Department of Transportation
Highway Division
Phoenix, Arizona

for

Research Project - Arizona HPR-1-15(164)

Sponsored by

The Arizona Department of Transportation
in cooperation with
The U.S. Department of Transportation
Federal Highway Administration

Arizona Transportation and Traffic Institute
College of Engineering
The University of Arizona
Tucson, Arizona

January 1978

1. Report No. FHWA-AZ-RS-77-164	2. Government Accession No.	3. Recipient's Catalog No.
4. Title and Subtitle Final Report - Phase I Testing Methods for Asphalt-Rubber		5. Report Date January 1978
		6. Performing Organization Code
7. Author(s) R. A. Jimenez		8. Performing Organization Report No.
9. Performing Organization Name and Address Arizona Transportation and Traffic Institute College of Engineering University of Arizona Tucson, Arizona		10. Work Unit No. (TRAIS)
		11. Contract or Grant No. HPR-1-15(164)
12. Sponsoring Agency Name and Address		13. Type of Report and Period Covered Final May 1976 - January 1978
		14. Sponsoring Agency Code

15. Supplementary Notes Prepared in cooperation with the U.S. Department of Transportation, Federal Highway Administration from a study Testing Methods for Asphalt-Rubber. The opinions and conclusions are those of the author and not necessarily of the Federal Highway Administration.

16. Abstract

The study is concerned with laboratory testing of an asphalt and rubber (A-R) mixture with special emphasis towards its use to minimize reflection cracking. Tests on the A-R blend showed that it had higher viscosity at high temperature and lower viscosity at low temperature than did the base 120 pen asphalt. Ductility values at 25, 12.7 and 0.5°C ranged from 16 to 29, thus showing good low temperature ductility. Two special tests were developed to compare A-R and RC-250 as tack coats and acting as strain attenuating layers (SAL). A-R was shown to be effective as a SAL in the "horizontal shear test," a static load test. The other new test, a repeated beam deflection test (vertical shear test) was capable of separating the test-response of the A-R and RC tack coats but not for the various application rates of A-R.

17. Key Words Asphalt-rubber, rubberized asphalt, asphalt testing, reflection cracking.	18. Distribution Statement No restrictions. This document is available to the public through the National Technical Information Service, Springfield, Virginia 22161

19. Security Classif. (of this report) Unclassified	20. Security Classif. (of this page) Unclassified	21. No. of Pages 91	22. Price

Form DOT F 1700.7 (8-72)   Reproduction of completed page authorized

Final Report - Phase I

TESTING METHODS FOR ASPHALT-RUBBER

Abstract

This report is concerned with laboratory testing of an asphalt and rubber mixture. The blend is called asphalt-rubber since the amount of rubber used and the characteristics of the blend are quite different than those reported in the asphalt paving literature. Tests performed on a blend of asphalt-rubber were (a) ductility with variable elongation rate and temperature, and (b) absolute viscosity with variable temperature.

The major portion of the study was devoted to developing equipment and test procedures for evaluating the use of asphalt-rubber as a strain attenuating layer to minimize reflection cracking in asphaltic concrete. Two test procedures were used to obtain the response of the asphalt-rubber layer when subjected to an increasing axial shearing force and also to a repeated transverse shearing force. Variables in the axial shear test were thickness of asphalt-rubber layer, thickness of overlay, and extension rate; while the variables for the transverse shear were thickness of asphalt-rubber layer, thickness of overlay, amount of the repeated transverse force (by deflection) and temperature.

The results of the testing program are used to discuss the possible reasons for the successful use of asphalt-rubber as a strain attenuating layer in asphalt overlay or new construction.

INTRODUCTION

Arizona, as well as many other states, has experienced the frustration of overlaying a cracked pavement with asphaltic concrete which subsequently shows the effects of reflection cracking. A reflection crack is one that develops in an overlay and which is directly over a preexistent crack in its supporting layer. The supporting layer may have cracked from shrinkage stresses, load stresses, or from the reflection crack phenomenon; this supporting layer may be composed of portland cement concrete, asphaltic concrete, cement treated base, or a clay bound soil course.

The mechanism leading to the development of a reflection crack is not completely understood. However, a certain amount of knowledge and experience are available to recognize the contributions of the tensile stresses caused by the restraint at the interface when the two layers undergo thermal shrinkage and also the shear and flexural stresses that develop as a wheel rolls from one side to the other of the preexisting crack of the supporting layer.

Naturally, we consider all surface cracks as contributing distress to a pavement.

Several solutions to the reflection cracking problem have been offered; and at one time or other have been found to be successful but not often enough or economical enough to receive wide acceptance. One of the approaches used has been to resist the differential movement between the two layers with the strength of the overlay. The strength of the overlay was achieved with layer thickness or with reinforcement

2

of wire mesh. Another approach has been to provide a yielding or "strain-relieving" layer between the old cracked layer and the new overlay, or the overlay itself was of such a pliable nature that deformations resulting from "crack" movements yielded low stresses without fracturing the surface layer.

"Asphalt-rubber" is a mixture of asphalt and fine grindings from rubber tires. It was developed and patented by C. H. McDonald in the early 1960's. In 1966, McDonald (1) reported early experiences with asphalt-rubber as a patching material for alligator type failures. Subsequent use of the asphalt-rubber as the binder for chip seal construction has shown that old pavement cracks have not appeared after at least 6 years of service. Olsen (2) has discussed the construction of asphalt-rubber chip seal coats with McDonald's binder of 25 percent rubber and 75 percent asphalt.

At the 1976 annual meeting of the Transportation Research Board, Morris and McDonald (3) presented a discussion on the use of asphalt-rubber to prevent reflection cracking. Examples of using the asphalt-rubber as a surface "stress absorbing membrane" (SAM) and also prior to overlay as a "stress absorbing membrane interlayer" (SAMI) are presented in the report. Because of the high rubber content, and the swelling and the softening of the rubber particles, the authors state that "...it is postulated that the asphalt is serving to modify the elastic properties of the rubber rather than the rubber serving to modify the characteristics of the asphalt."

The asphalt-rubber mixture has been used largely on an ad hoc basis and as such no laboratory tests or measurements have been made to characterize its behavior as a strain attenuating layer. The

objectives of this study were to investigate established procedures or develop new ones to characterize certain physical properties of a particular asphalt-rubber blend and also to characterize the blend's capability to serve as a strain attenuating layer to preclude reflection cracking.

ASPHALT AND RUBBER MIXTURES

The mixture of asphalt and rubber used in this study was held constant as to the amount and type of the two components. The material to be more fully identified later was a combination of a relatively soft asphalt cement and particles (#16-#25 sieve) of rubber from passenger tires; the proportion was 3 parts of asphalt to 1 part of rubber by weight basis. The mixture was specified by the Arizona Department of Transportion (ADOT) and has been labeled asphalt-rubber in opposition to rubberized asphalt. Although the asphaltic blend was not a variable in the study, a brief review of rubber in asphalt is deemed necessary to develop an understanding and significance of the jargon and factors affecting the behavior of mixture of rubber and asphalt.

The addition of rubber to asphalt would seem to be desirable since it would be expected to improve elasticity and low temperature flow properties of asphalt (4,5,6,7,8). In 1898 Caudenberg obtained a patent for a process to manufacture a rubberized asphalt (4). Of course, at that time the additive was a natural rubber. Since then various methods have been used to blend various types of natural or synthetic rubbers with asphalt. These different rubbers are described as follows:

1. Natural rubber is made from the milky sap of the rubber tree which was discovered in South America. Natural rubber is quite temperature susceptible and ages quite rapidly.

2. Vulcanization is a process for combining sulfur with natural or synthetic rubber to reduce temperature susceptibility and

improve other characteristics desirable for pneumatic tires.

3. Synthetic rubber was developed during World War II from petroleum. Although there are many types and grades of synthetic rubber, the most common type used in the manufacture of tires in a copolymer of styrene and butadiene abbreviated SBR (8).

4. Reclaimed rubber is a product from the treatment of vulcanized scrap tire rubber--"whereby a substantial "devulcanization" or regeneration of the rubber compound to its original plastic state is effected, thus permitting the product to be processed, compounded, and vulcanized." (9).

5. Rubber latex is a suspension of rubbery particles as an emulsion in water. If of natural rubber, the particles are of colloidal size and contain 20-40 percent solids; if of synthetic rubber, the solid content may be from 20-70 percent (9).

Dispersion of Rubber in Asphalt

The literature reviewed has generally been concerned with small quantities (less than 5 percent by weight of asphalt) rubber and the size of rubber particles has not been specified. When rubber was introduced as a liquid latex, one would have to assume that rubber particles would pass through a #200 mesh sieve (0.003 inch or 75 micron). If the rubber was in a granule, crumb or powder form, then one would have to assume that the size range of these was from 0.30 inch (7.6 mm) to 0.03 inch (0.08 mm) but not the complete range for any one of the forms. There is somewhat general agreement that the rubber is not soluble in asphalt (8,9); however, a submicroscopic size particle or even an individual molecule could go into solution (4,10).

The dispersion of rubber in asphalt is usually accomplished at elevated temperatures of 280°F to 375°F (138°C to 190°C) with moderate agitation for a specified period of time. Under optimum conditions a specific particle size may increase in volume (swell) by a factor of up to 5 for natural rubber (4). The dispersion of the rubber particles to produce the desired improvements in the asphalt may be affected by the following:

1. Mixing temperature - usually detrimental if held too long above 420°F (216°C) (8)

2. Duration of mixing time. The effect is also dependent on temperature; however, the effect becomes constant after a minimum time (4)

3. Stirring shear--break down of rubber if too high (8)

4. Particle size and its distribution

5. Type and quantity of rubber (4)

6. Amount of aromatic (cyclics) component in the asphalt (8)

The review presented in the previous paragraphs was related principally to blends characterized as rubberized asphalt since the rubber content was relatively low and visual appearance of the blend was that of asphalt.

The literature on asphalt-rubber blends containing 20 percent or more of rubber is extremely limited. LaGrone et al (9) refers to a blend containing 20 percent reclaimed rubber but does not present properties of this material. Characterizations of high rubber content blends are presented by Morris and McDonald (3) Green and Tolonen (11), Frobel, Jimenez, and Cluff (12) and Kalash (13). The laboratory findings of these four reports (3,11,12,13) are related principally

to a blend of 3 parts AR1000 asphalt with 1 part passenger tire rubber having a size range between the 16 to 25 mesh sizes (1.2-0.7mm) and can be summarized as follows:

1. The effect of the rubber was to increase the viscosity at temperatures above ambient and reduce the temperature susceptibility.

2. The ductility value at $77^{O}F$ ($25^{O}C$) was reduced by the addition of rubber (12,13).

3. The flow value for the Barrett Slide Test was reduced (12).

4. The tensile pullout toughness value by the Benson procedure was increased by the addition of rubber (12).

As can be seen from the above not much laboratory information is available which can be used to predict the performance of the asphalt-rubber as a strain attenuating layer (SAL).

The next sections describe tests and results obtained from measurements made on the binder by itself and also when serving in a mode simulating a strain attenuating layer.

MATERIALS AND TESTS PROCEDURES

In this study the materials used were not to be varied; however, certain measurements had to be made to characterize these in terms of standard technology.

Materials

Asphalt

The low viscosity asphalt of this AR1000 grade (14) and the rubber additive were furnished by the Arizona Department of Transportation (ADOT) in sufficient quantities to eliminate a batch variable. The asphalt properties are shown in Table A1 in Appendix A; although the table does not contain information on the asphalt's composition, it has been determined that the aromatics (cyclics) component content was of a satisfactory amount and type.

Rubber

The data appearing in Table A2 show that the particle size distribution of the rubber was such that ninety-nine percent passed the No. 16 (1.2mm) sieve, twenty percent passed the No. 30 (0.6mm) sieve, and two percent passed the No. 50 (0.3mm) sieve. The table also shows that soaking the rubber in benzene to cause the particles to swell and then drying at $140^{\circ}F$ ($60^{\circ}C$) did not change appreciably the dry size of particles.

9

Asphaltic Concrete

In order to minimize the effects of storage time on the physical properties of beams to be made of asphaltic concrete, a proven procedure was used. A large quantity of asphaltic concrete was obtained from a commercial plant and stored in sealed 5-gallon (19 l.) metal cans. When material was needed for making specimens, a can was placed in a $180^{o}F$ ($82^{o}C$) oven for 1-2 hours. After this period of time, the mixture was soft enough for sampling. Care was taken in keeping track of the weight of the mixture in the cans so that a can would not be heated in the $180^{o}F$ ($82^{o}C$) oven more than twice.

After obtaining the desired weight of sample, it was heated in a $250^{o}F$ ($121^{o}C$) oven in preparation for compaction. Compacted specimens were then stored in a room maintained at $77^{o}F$ ($25^{o}C$) for periods ranging in time from a minimum of three days to as much as fourteen days. Prior work (15) had indicated that this procedure was satisfactory for minimizing the effects of storage time.

Two paving mixtures were obtained from a local hot-mix plant. A mixture labelled "3/4" Tanner" was obtained for the testing sequence related to loadings of horizontal shear forces at the interface between an old pavement and a new overlay. Characteristics of this mixture are shown in Table A3 which shows test values for density, Hveem stability, and cohesiometer value for specimens compacted by two procedures. It is noted that the density of beams compacted in one layer or two layers is given for comparison with the density of 4-inch (101mm) diameter specimens.

Test Procedures

As indicated earlier the project's goal was to develop test procedures related to reflection cracking; however, viscosity and ductility tests were performed to obtain comparative values for the straight asphalt and the asphalt-rubber.

Prior to performing any test on the asphalt-rubber it is necessary to blend the two materials. As indicated by Endres (8) and Green et al (11) the characteristics of the asphalt-rubber are dependent on the mixing procedure. The equipment, temperature, and duration used to make the blends are detailed in Appendix B.

Viscosity Test

Viscosity tests were performed over a range of temperatures from $59^{\circ}\text{-}104^{\circ}\text{F}$ ($15^{\circ}\text{-}40^{\circ}\text{C}$) using a falling coaxial cylinder viscometer. Cylinders and pistons were fabricated to satisfy that ratio of annulus width/length being less than 0.5 as recommended by Traxler and Schweyer (16).

The annulus width of the viscometer was set at 1/4 inch (6.3mm). This value was selected on the basis that the diameter of a tube should be at least five times larger than the maximum particle size of a mixture to be forced through it. If the dry rubber passes the No. 16 (0.05 in.) and swells by a factor of five according to Endres (8) or a factor of two according to Green (11) then the largest particle in the asphalt-rubber would be between 0.10 to 0.25 inch (2.5-6.3mm). Recalling that the swell factor of five was for a natural rubber, we preferred to select the swell factor of two in order to obtain a tube diameter of 0.5 inch (12.7mm) or the annulus width of 0.25 inch (6.3mm).

Photographs of the viscometers and the set-up for testing in a
water bath, sample preparation, and the test procedure are described
in Appendix C.

Ductility Test

Variations of the standard AASHTO ductility test were performed
at temperatures of 33°, 55°, and 77^OF (0.6, 12.8, and 25^OC) and at
extension speeds of 5, 11, and 19 centimeters per minute. Data for the
asphalt and asphalt-rubber are listed in Table 6A.

Beam Tests

It is pointed out at the onset that the testing was not exactly
as implied by the word "beam" since the asphaltic concrete specimen was not
spanning a large clearance. (See page 89.)

The composite beam was made up of two 6 x 20 x 1/2-inch (152 x 508 x
12.7mm) aluminum plates and an asphaltic concrete specimen 5 x 12 x 2
or 4-inch (127 x 305 x 51 or 101mm). The two aluminum plates butted
to within 1/32-inch (0.8mm) of each other and were joined with a tack
coat and the asphaltic concrete beam. The procedure for making the
asphaltic-aluminum beam is described in Appendix D.

Horizontal Shear Test. This test was used to simulate the hori-
zontal stress that occurs at the interface of an overlay and at the
crack of an old pavement that is undergoing cooling.

Appendix E contains a detailed description of the test. A review
of the procedure will show that one of the aluminum plates was pulled
away from the other one and that a "horizontal" shear force was carried
by the tack coat to the asphaltic concrete specimen, The principal
measurements made were the shear force and the amount of slip between

the aluminum plate and the asphaltic concrete specimen as a continuously increasing load was applied. As noted three rates of loading were used and the tack coat was also a variable.

Vertical Shear Test. The test as described in Appendix F was developed to simulate a repeated wheel load being transmitted from one side of a crack to the other side by an overlay course.

Briefly, the test procedure involved the repeated application of a deflection to one end of an aluminum plate and establishing the number of repetitions required to crack the asphaltic beam. The main variables of the experiment were as follows:

a. amount of deflection--3 levels

b. tack coat--4 levels

c. temperature--2 levels

d. asphaltic concrete thickness--2 levels.

RESULTS AND DISCUSSION OF TESTS

The results of the tests performed are listed in the table of Appendix A. However, pictorial presentations and additional tabulations will appear in the text of this section.

In general the discussion will be centered on indicating the differences in response to tests between straight asphalt and asphalt-rubber.

Materials

Asphalt Cement and Rubber Fines

Tables A1 and A2 of Appendix A show the standard measurements made on the two materials. It is noted that the asphalt is of relatively low viscosity especially if it were to be used in a surface course in southern Arizona.

The measurements for gradation were made to characterize the particle size distribution of the rubber fines. However, of some interest are the measurements made after soaking in benzene to cause swelling of the particles and then drying for sieve analysis. The data of Table A2 indicate the swelling of the particles by soaking in benzene is similar to the swelling of a sponge when it soaks water and then shrinks when dried. This would seem to indicate that the swelling phenomenon of the rubber particles was primarily a physical one.

14

Asphaltic Concrete

The data of Tables A3 and A4 are presented to show characteristics of the mixtures and to show certain comparisons between the two compactors and the two types of specimens made.

The important comparisons to show are that the procedure developed for the compaction of beams did produce densities that were comparable to those of the 4-inch (101mm) diameter ones and also that A-R tack coats did not affect the density of beams compacted on them.

Viscosity Measurements

Viscosity measurements made on the asphalt cement and asphalt-rubber are presented in a somewhat different form that appears in the literature. Usually viscosity for asphalts is given at one specified shear rate and so the shear stress-shear rate relationship is not apparent. Table 5A presents information for describing the shear stress-shear rate relationship for asphalt cement and also asphalt-rubber at various temperatures. Also since the equations were developed statistically, the coefficient of correlation, R^2, is shown; note the particularly high values (.85-.99) obtained for the asphalt-rubber especially since the method for casting the test specimens was not a standard one.

Table A5 also shows the viscosities calculated at a shear rate of 5×10^{-2} reciprocal seconds. These viscosities were used to determine the best-fit line between viscosity and temperature using linear models of log viscosity-log^{o}F and also log log viscosity-log^{o}R (Rankine). The complete equations and coefficient of correlation for each are listed on Table 1. Using the logη-log^{o}F equations from Table 1

Table 1. RELATIONSHIP BETWEEN VISCOSITY (η) AND TEMPERATURE FOR ASPHALT CEMENT AND ASPHALT-RUBBER*

Material	Model	Equation	n	R^2
Asphalt Cement	$\eta = IF^b$ $(F={}^{\circ}F)$	$\eta = 6.767 \times 10^{25} F^{-10.69}$	5	0.999
	$\mathrm{Log}\, \eta = IR^b$ $(R={}^{\circ}\mathrm{Rankine})$	$\mathrm{Log}\, \eta = 3.422 \times 10^{16} R^{-5.781}$	5	0.999
Asphalt-Rubber	$\eta = IF^b$ $(F={}^{\circ}F)$	$\eta = 5.768 \times 10^{14} F^{-4.494}$	5	0.925
	$\mathrm{Log}\, \eta = IR^b$ $(R={}^{\circ}\mathrm{Rankine})$	$\mathrm{Log}\, \eta = 7.597 \times 10^{6} R^{-2.227}$	5	0.951

*Viscosity determined at a shear rate of 0.05 sec.$^{-1}$ for regression analysis.

for both materials, viscosities for three temperatures are calculated and shown below.

Temp. $^{\circ}$F($^{\circ}$C)	32(0)	77(25)	140(60)
Asphalt η, p.	550×10^6	460×10^3	774
A-R η, p.	99×10^6	1.92×10^6	131×10^3

The above values of viscosity show that at the higher temperature the asphalt-rubber has much higher viscosity than the asphalt but at the lower temperature the opposite is true; and of course, this lower temperature susceptibility of the asphalt-rubber is very desirable. (The calculated viscosity of the asphalt at 140°F (60°C) compares favorably with the measured value of 744 p. shown in Table A1).

Ductility Value Measurements

The standard AASHTO ductility test for asphalts was modified with reference to speed of elongation and temperature conditions. These variations were made to obtain comparative measures for the deformability of the asphalt-rubber.

Table 6A of Appendix A shows that the AR-1000 asphalt stretched the full distance of the device for all three speeds with the two higher temperatures; however, the ductility value was zero for all three speeds with the test temperature of 33°F (0.5°C).

The asphalt-rubber specimens did not show much response to the speeds or temperatures used in that the total range of values was from 16 to 29; even for the lowest temperature the values were from 16 to 22.

It was noted that there was not much dimensional reduction in the transverse direction while the test was underway and then some of the reduction was recovered after fracture.

Again, we note the better low temperature response of the asphalt-rubber.

The reduced value of ductility for the asphalt rubber at 77^OF (25^OC) is contrary to the findings of others (7,8) when small amounts· of latex are used to make rubberized asphalt. The reduced elongation of the asphalt-rubber is attributed to the consideration that the rubber particles are behaving as elastic aggregate in the blend. Under this condition, it is anticipated that the asphalt-rubber blend may have a reduction in cohesion and adhesion values as compared to those of the straight asphalt.

Horizontal Shear Test

As mentioned earlier, the variables in this part of the experiments were (a) rate of loading, (b) asphalt beam thickness, and (c) amount of A-R tack coat. The zero level of tack coat was actually a tack of RC-250 applied at a rate of 0.05 gallon per square yard.

The question may arise as to whether or not the aluminum plate can be said to represent an actual pavement surface. Also as mentioned earlier, this test examines the capability of the tack coat to transfer the shear force from the aluminum plate to the asphalt beam. Repeated examination of the failed specimens showed that for the RC-250 tack coat fracture occurred at the beam interface and for the A-R tack coats fracture occurred within the tack-coat. Since at no time did fracture occur at the aluminum plate interface, then the objectives of the test were reached.

The data for the horizontal shear test appear in Tables 7A and 8A of Appendix A. The numerical values shown in the table were obtained

from plots of load and slip versus time as shown in Figures 1 and 2. From Figure 1 for the R-C tack coat it is evident that fracture occurs at the maximum load applied. However, examination of Figure 2 shows that an ultimate amount of load is maintained for awhile as the rate of slip increases until fracture of the A-R tack coat results from shear. This last behavior was not noticed when the first A-R beams with 0.6 g.s.y were tested and as a result the loading was stopped as soon as it started to decrease as was done with the beams tacked with RC-250. It will be noted that the measurements for slip at rupture and load at slip rupture are not available for the 0.6 g.s.y. A-R beams.

The general indications of the data obtained for this test are that the A-R tack coat is stronger than the RC-250 at low deformation rates but weaker at high deformation rate; however, the extensibility of the A-R tack coat is much greater than that of the RC-250 and its value increases with an increase of deformation rate.

The next three figures show comparisons between A-R and RC-250 data. Figure 3 shows the effects of extension rate and amount and kind of tack coat on the maximum load obtained in the horizontal shear test. It is seen that the A-R tack coats are less susceptible to rate of loading and that the strength of the A-R tack coat decreases as the thickness (application rate) increases.

Figure 4 shows the effects of extension rate on the amount of slip occurring at maximum load; however, at maximum load, failure or rupture of the A-R tack coat has not occurred. Note that the effects of type and amount of tack coat are opposite to those shown in Figure 3, that is, for RC-250 the amount of slip decreases as the extension rate increases and the amount of slip increases as the amount of A-R increases.
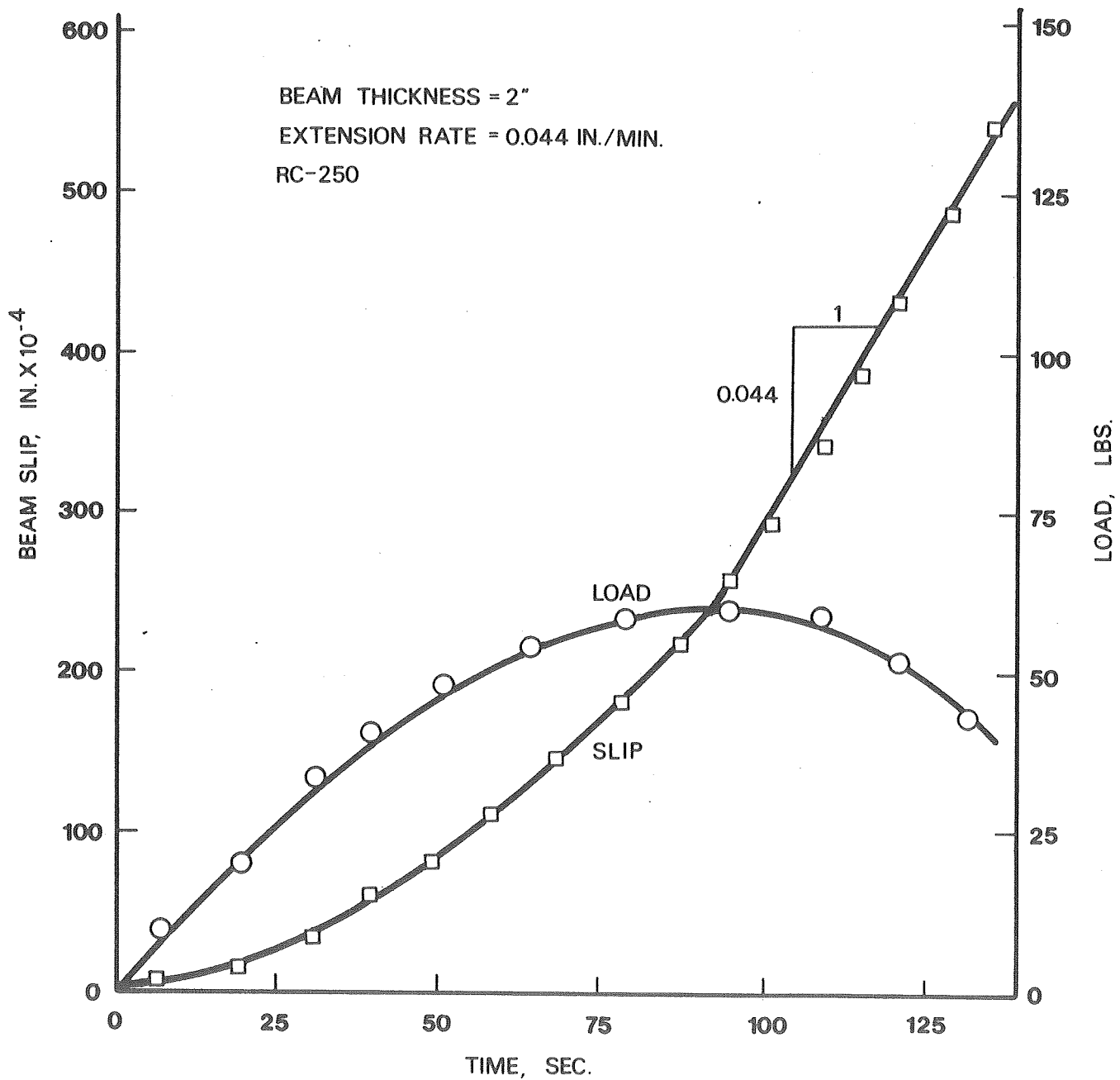
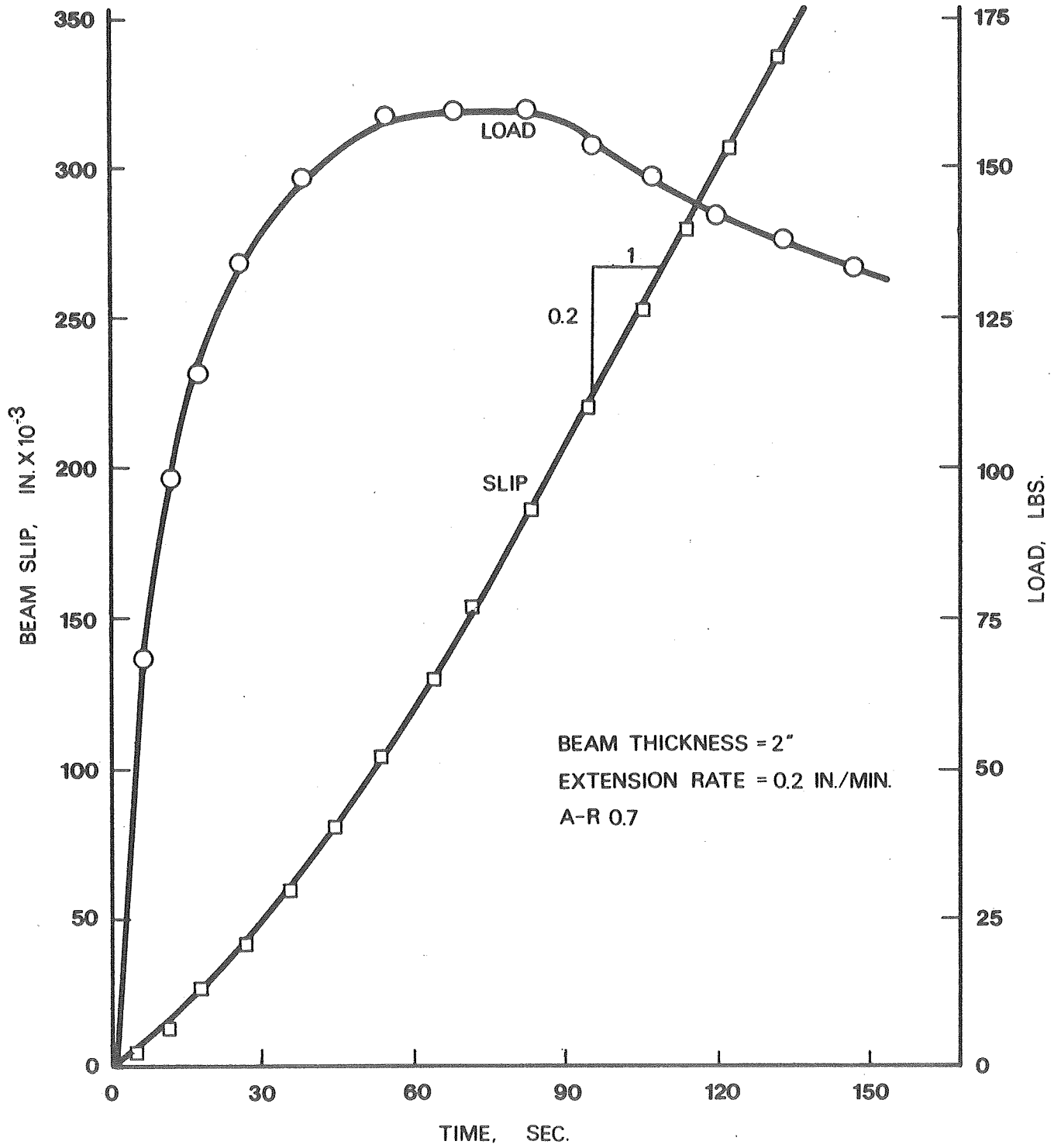Figure 1. Typical Plot of Load and Slip vs. Time for RC-250 Tack Coat

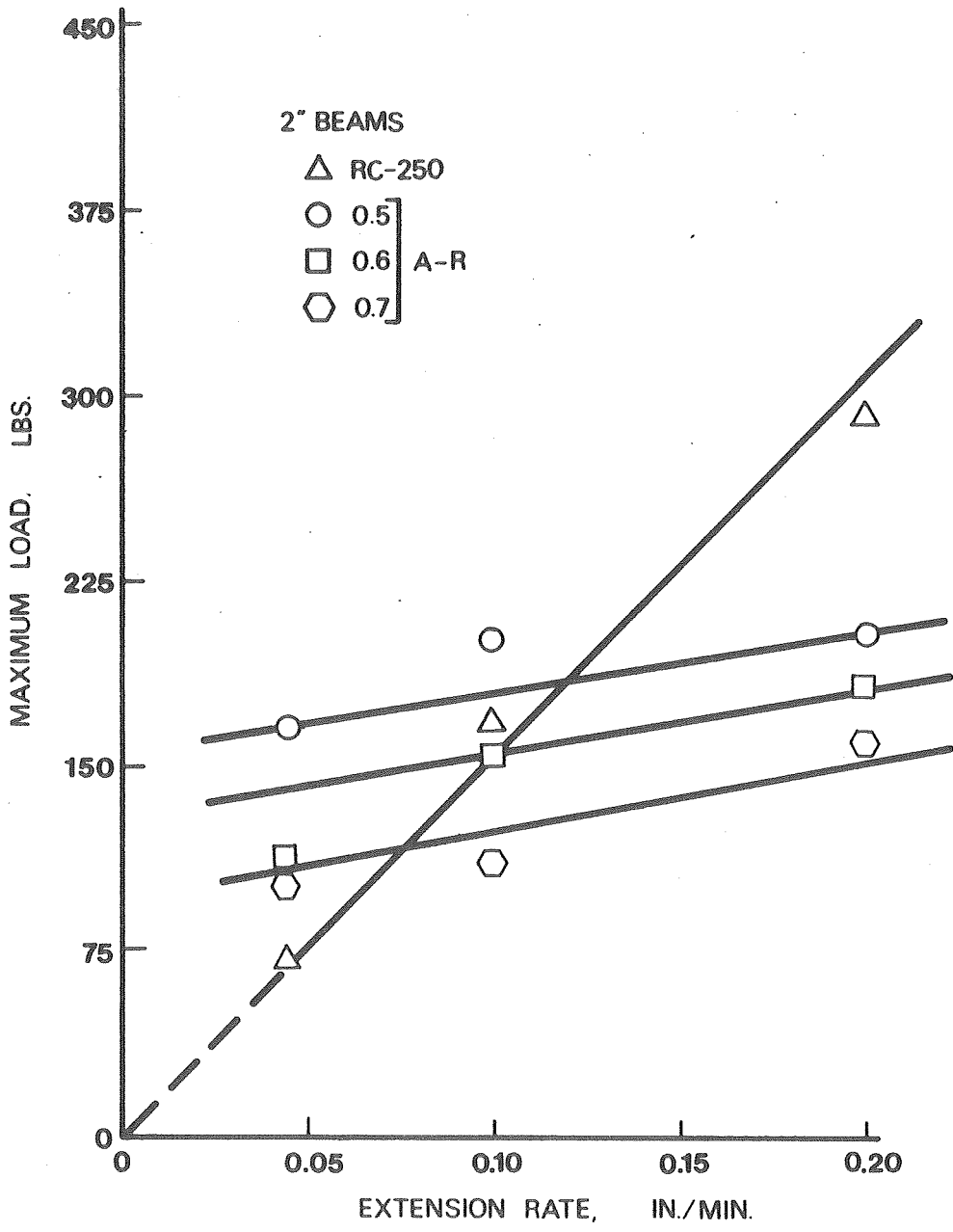Figure 2. Typical Plot of Load and Slip vs. Time for A-R Tack Coat

Figure 3. Relationships between Maximum Load and Extension Rate
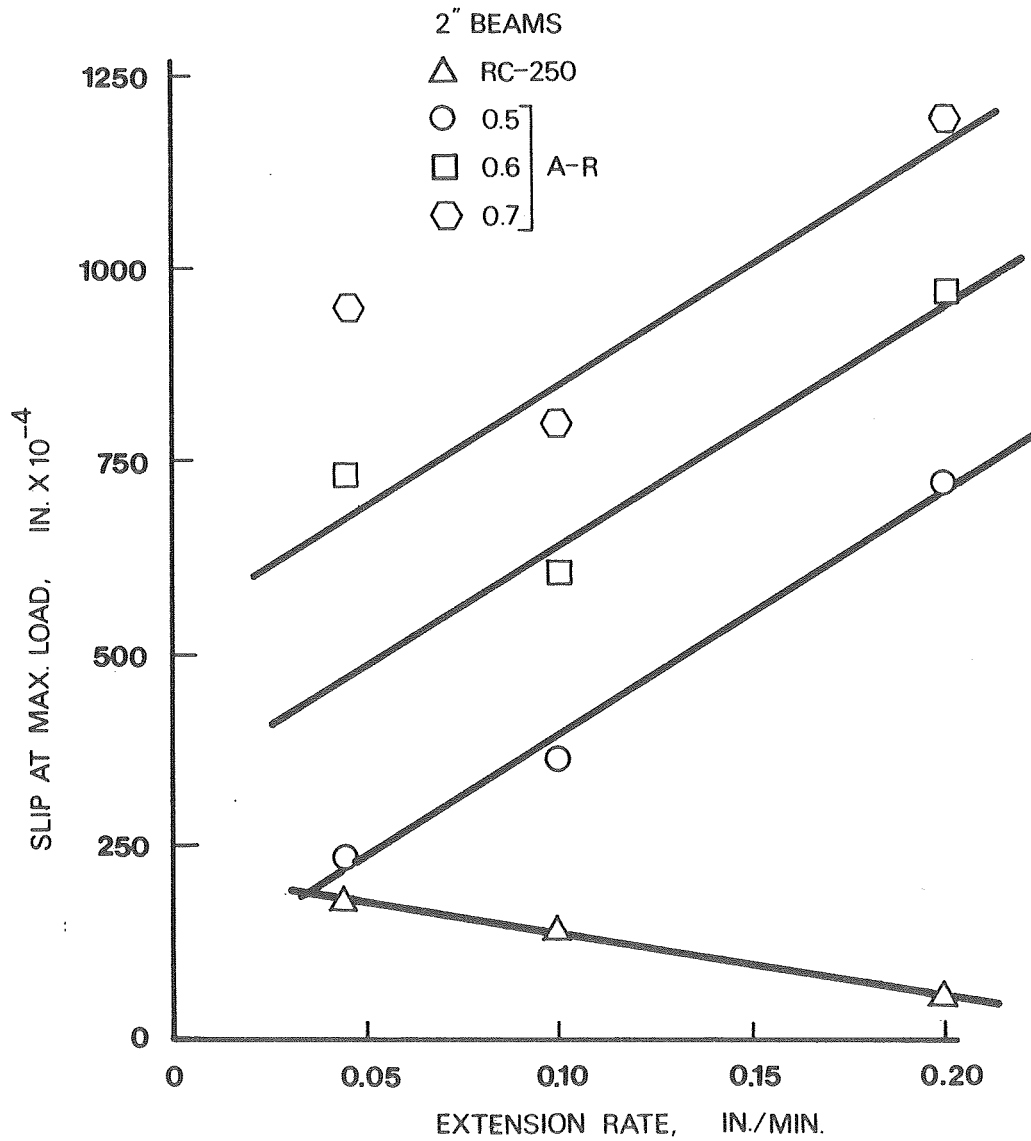in the Horizontal Shear Test for RC-250 and A-R Tack
Coats

Figure 4.   Relationship between Slip at Maximum Load and Extension
Rate in the Horizontal Shear Test for RC-250 and A-R
Tack Coats

A composite of Figures 3 and 4 to show the significant and great differences in response to the horizontal shear test between the RC-250 and A-R tack coats is presented in Figure 5. The curves show the reason for the A-R tack coat to serve as a strain attenuating layer in that large strains (slip) result in relatively small loads being transmitted by the SAL in comparison to the standard use of RC-250 as a tack coat.

The above figures and discussion have been related to beams 2 inches (51mm) in thickness. The comparison between RC-250 and A-R tack coats on 4-inch (101mm) beams for maximum load and slip at maximum load are similar to those for the 2-inch (51mm) beams. However, the effects of amount of A-R were not as directional as for the 2-inch (51mm) beams. Examination of Table 8A and Figure 6 shows that the maximum load for the 4-inch beams was greater than for the 2-inch beams at 0.5 and 0.7 g.s.y A-R for all of the extension rates. However, the value of slip at the maximum load was greater for all of the 2-inch beams. It then becomes apparent that the performance of the A-R as a strain attenuating layer with regards to horizontal forces is maximized at the lower thickness of overlay and at the greater application of A-R. It is also noted that the extensibility of the 4-inch beam with 0.7 g.s.y. A-R is greater than that for the 2-inch beam with 0.5 g.s.y. A-R. The data are not extensive enough to optimize beam thickness with the application rate of the A-R tack coat but the data do imply that as the overlay thickness is increased then the A-R application rate should also be increased.
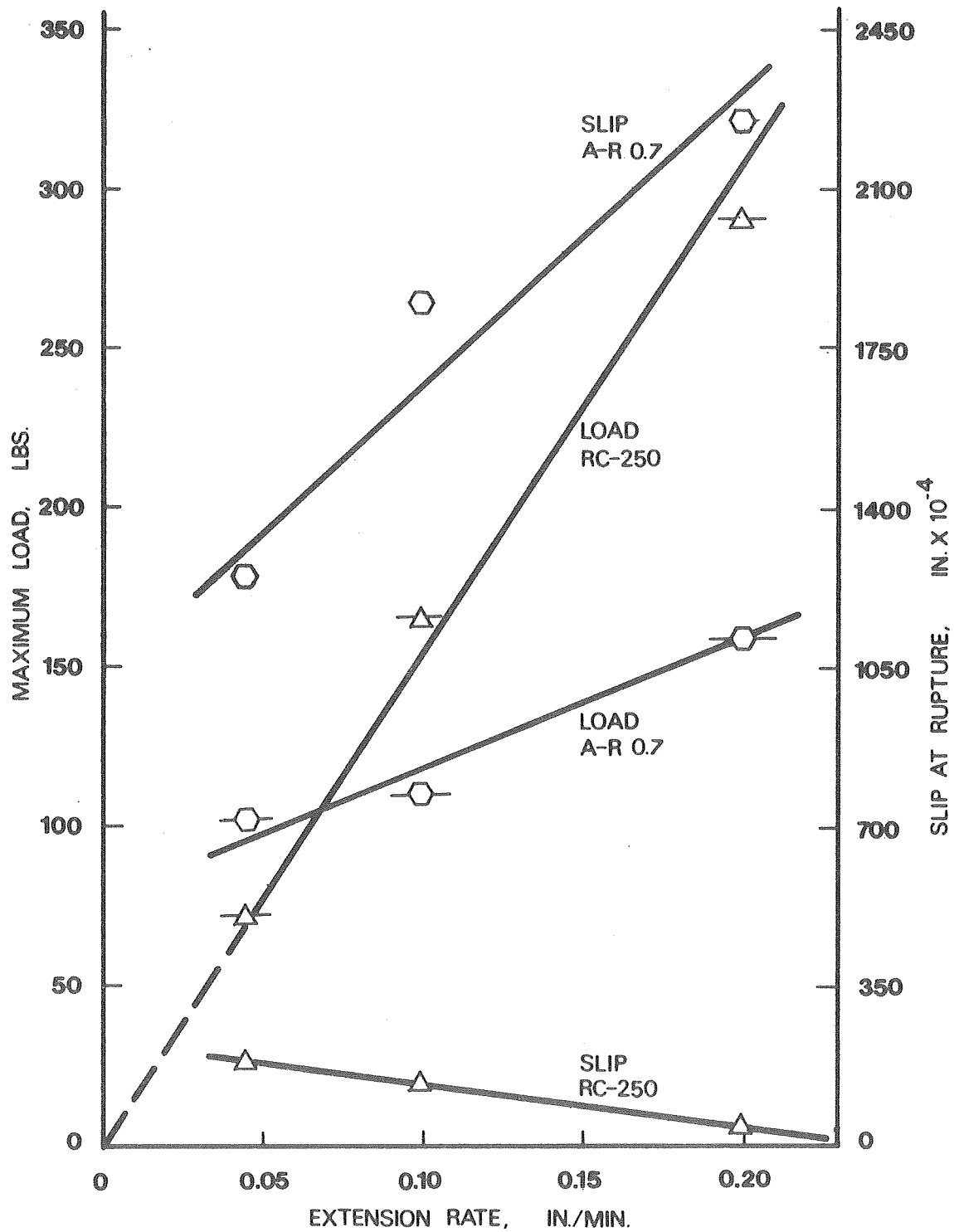
Figure 5. Comparison of Load and Slip Responses for RC-250 and A-R Tack Coats in the Horizontal Shear Test
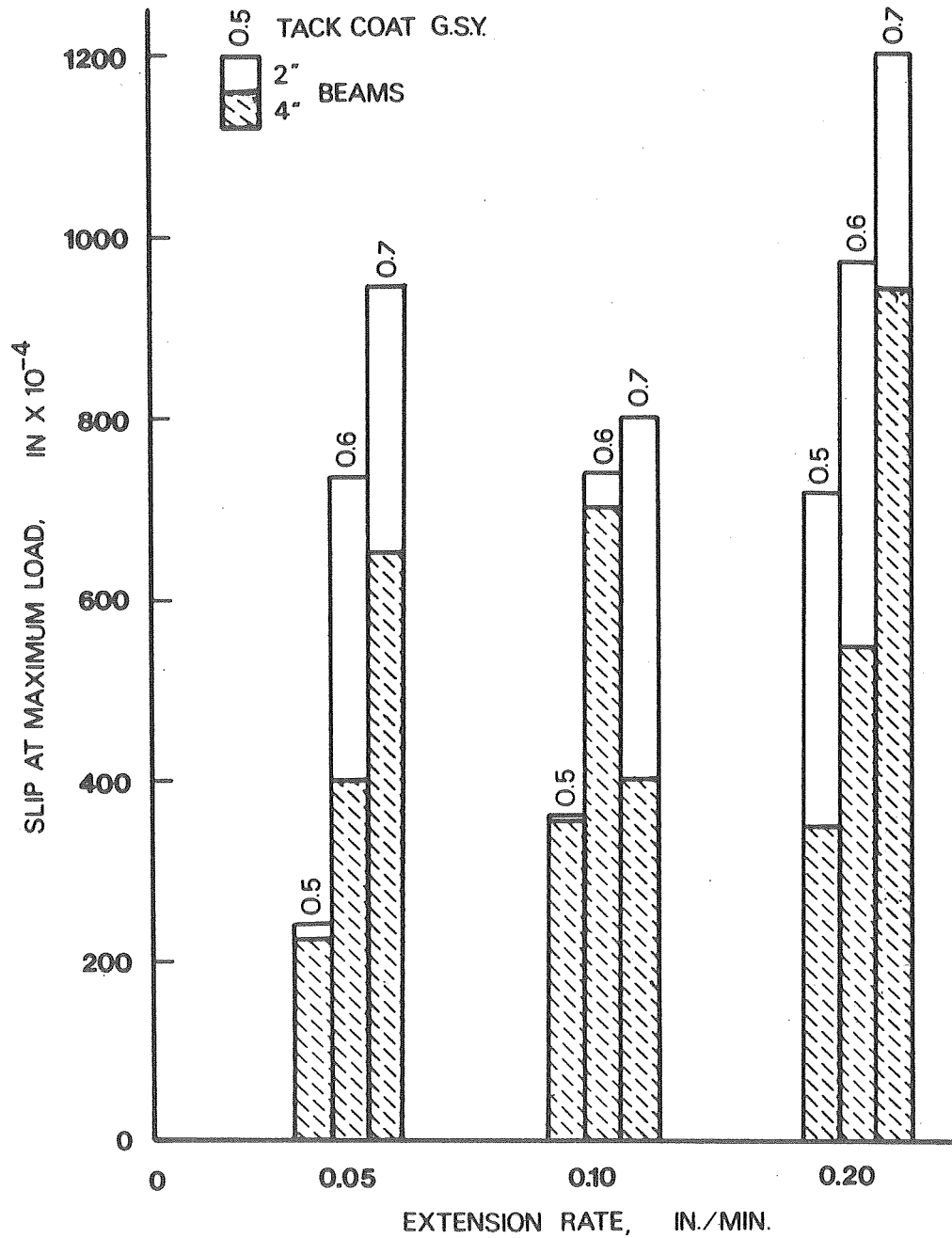
Figure 6. Effects of Beam Thickness and Amount of A-R on Slip in the Horizontal Shear Test

Vertical Shear Test

The vertical shear test was devised to simulate the condition resulting when a wheel load is transferred from one side of a crack to the other by means of an overlay. Field measurements for studies of reflection cracking have been principally the deflections near a crack under load (17,18). For this reason, the test was designed for inducing repeated deflections at the joint of the laboratory prototype of a pavement. The principal variables to be related to number of deflection repetitions causing failure of the beam were (a) amount of tack coat, (b) thickness of beam, and (c) test temperature. The data obtained from the testing program appear in Table 9A and 10A of Appendix A.

As described in the procedure, the response desired for a repeated deflection was the number of repetitions to cause a crack in the asphaltic concrete beam. Figure 7 shows various plots of deflection vs. repetitions to failure. It is noted that the plots are linear in the log-log coordinate system and that the 4-inch (101mm) thick beams have a longer "fatigue" life than the 2-inch (51mm) ones. It must be mentioned now that a greater force was required on the thicker beam to cause the same deflection as on the thinner one.

The linearity of all plotted data suggested the general model for relating deflection to repetitions in the following form:

$$\delta = I_o N^{-b}$$

where
δ is the repeated deflection

I_o is a constant,

N is the number of repetitions to cause failure
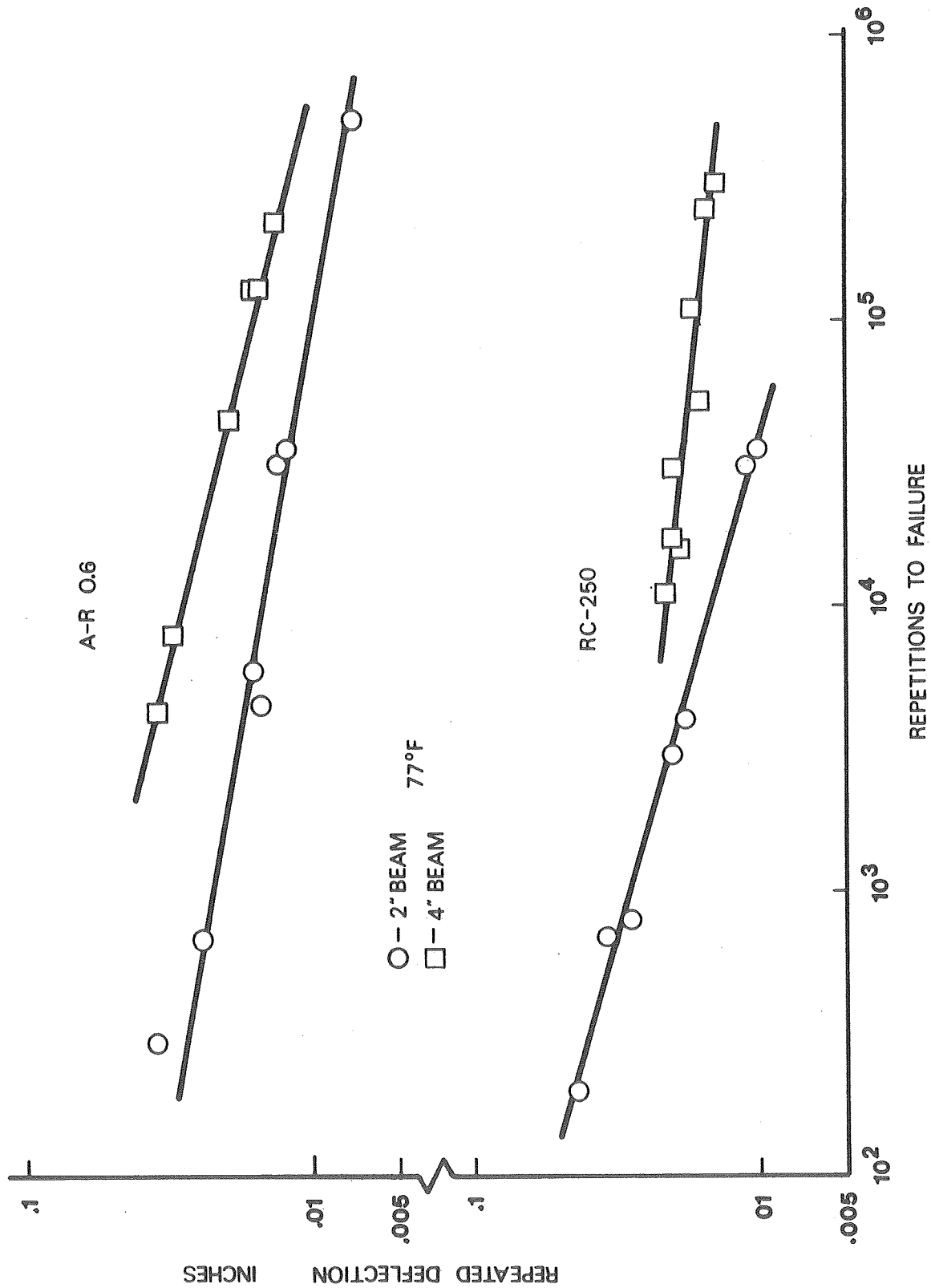
b is a constant.

Figure 7. Relationship between Repeated Deflection and Number of Repetitions to Cause Failure in the Vertical Shear Test

Evaluation of the constant I_o and $\underline{b}$ by means of a least-squares-fit yielded the values shown in Table 2. It is noted that the values for the coefficient of correlation R^2 are relatively high which indicates the acceptance of the model. As with any other model determined in the method mentioned, one must not attempt to use values extrapolated past the measured data. This is especially true for these data since there is a suspicion that an endurance limit may exist at deflections approaching 0.005 inch (0.13mm). Although only two sets of measurements (one in Table 9A and the other in Table 10A) are presented, during the initial testing with the device it was noticed that extremely long periods of time were required to fail a beam under small deflections.

Examination of the values for $\underline{b}$ in Table 2 for the 2-inch beams tests at 77^oF (25^oC) shows that there is not much difference among them. This suggests that there was no significant difference in the response of the beams with the different tack coats.

The effect of reduced test temperature on response of the beams can be estimated from the data for the RC-250 and A-R 0.6 specimens. From Table 2 it is noted that the slope of the log δ-log N curve, as described by the value of $\underline{b}$, decreases from 0.252 to 0.206 a difference of 0.048 for the A-R 0.6 beams while the difference in slope is 0.172 for the RC-250 beams. This reduction in susceptibility to temperature of the A-R beams goes along with the findings of the ductility test.

The effects of beam thickness on the response to the vertical shear test could not be explained in terms of the tack coat interaction. As a consequence, an elastic analysis of the testing system was performed. Professor DaDeppo of the Civil Engineering Department developed

TABLE 2. RELATIONSHIP BETWEEN REPEATED DEFLECTION, δ,
AND NUMBER OF REPETITIONS TO CAUSE FAILURE, N,
IN THE VERTICAL SHEAR TEST.

$$\delta = I_0 N^{-b}$$

Tack Coat	Temp.	I_0	b	n	R^2
		2" Beam			
RC-250		0.205	0.287	7	0.980
A-R 0.5	77°F	0.151	0.243	6	0.998
A-R 0.6	(25°C)	0.180	0.252	7	0.991
A-R 0.7		0.261	0.300	7	0.973
RC-250	38°F	0.060	0.115	7	0.943
A-R 0.6	(3.3°C)	0.134	0.206	8	0.987
		4" Beam			
RC-250	77°F	0.060	0.115	8	0.900
A-R 0.6	(25°C)	0.264	0.243	6	0.990

expressions for stresses within the composite beam assuming linear elasticity. This development is described in Appendix G.

A further effort for the evaluation of stresses in the composite system was to write a computer program for the calculation of deflections, flexural stresses, axial stresses, and shear stresses at different points in all three materials of the beam. It was not the intent to delve too deeply into the effects of material properties or dimensions on the stresses of the system since the analysis was based on linear elastic theory. However, a fixed set of material properties was used to see how thickness of the asphalt beam and thickness of the tack coat affected certain stresses in the system and then replace the corresponding stresses with deflection in the deflection-repetition fatigue relationship.

The first step to accomplish the above goal was to establish load-deflection relationships for various of the composite beams mounted on the vertical shear test device. The beams were loaded with a cable-bucket-falling shots system at a rate of 1200 grams per minute and deflection readings on the beams were taken at specified time intervals. Figure 8 shows the plotted load-deflection data for the beams loaded as described above. The curves of the plot give an indication of the linearity between load and deflection being affected by beam thickness or test temperature. The procedure used was not capable of responding to differences in the tack coat.

The deflection and beam component sizes were used to calculate the corresponding load with the results of the elastic analysis of the system for assumed values of moduli and Poisson's ratio. A comparison between the measured and calculated loads is shown in the curves of
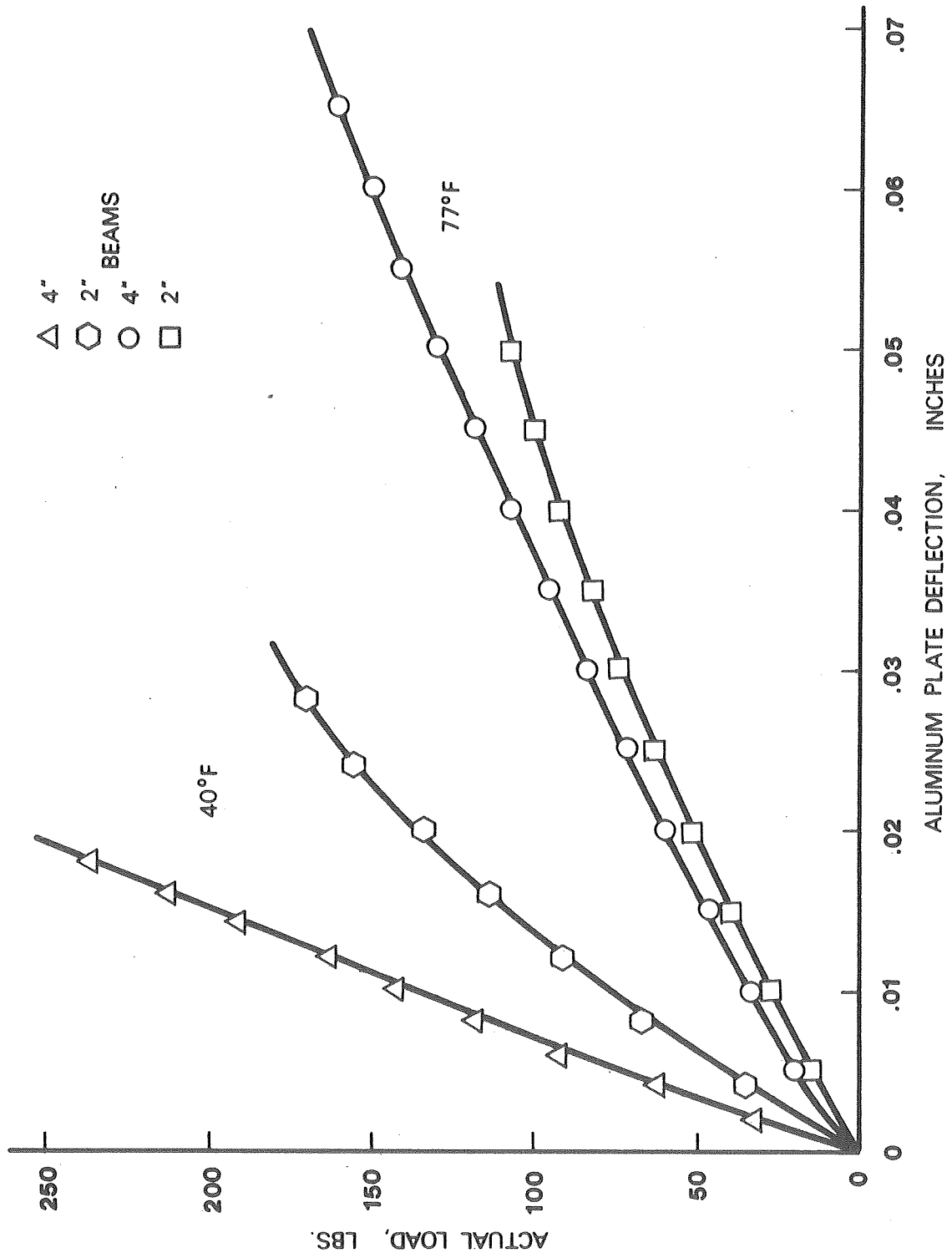
Figure 8. Relationship between Measured Force and Aluminum Plate Deflection for the Vertical Shear Test

Figure 9. The reader is reminded that the calculated load for a deflection is not affected by temperature as the measured load was; also the measured load was not affected by the amount of tack coat but the calculated load was. Our concern was not so much with the above considerations but more so with the linearity of the plotted data of Figure 9, for if the data deviated excessively from a straight line then the calculated stress could not be substituted for deflection in the deflection-repetition fatigue relationship. The plots shown in Figure 9 were assumed to be sufficiently linear and so certain stresses were calculated for a point above the crack (joint) and in the asphalt beam as well as in the tack coat assuming that the integrity of the beam was maintained up to the point of fracture. This assumption appears to be valid since the deflection across the crack was relatively constant up to the point of fracture.

The values of stresses calculated to replace deflection in the fatigue equation are shown in Table 3. Using the equations shown in Table 2, the number of repetitions to cause failure were calculated for deflections of 0.010 and 0.035 inch (0.25 and 0.89 mm). The measured loads to cause the above deflections were used to calculate tensile and shearing stresses above the joint in the tack coat and also the asphaltic beam. The following indicates the thickness of the corresponding application of tack coat:

> A-R 0.7 g.s.y equaled 0.125 in. (3.2 mm)
>
> A-R 0.6 g.s.y equaled 0.107 in. (2.7 mm)
>
> A-R 0.5 g.s.y equaled 0.089 in. (2.3 mm)

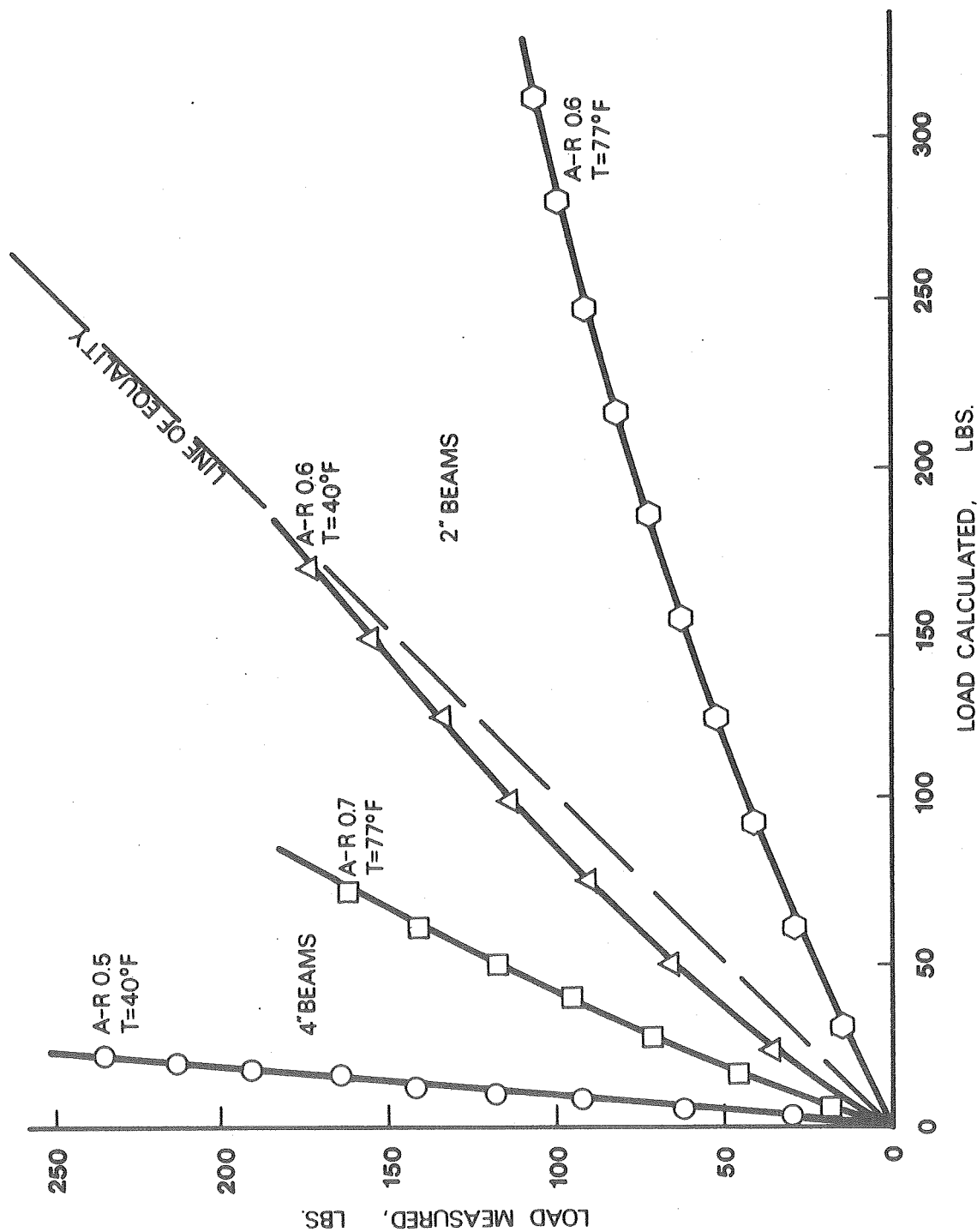RC-250 0.05 g.s.y assumed to equal A-R at 0.004 in. (0.10 mm).

Figure 9. Relationship between the Measured Force vs. the Calculated Force at Equal Deflections for the Vertical Shear Test

TABLE 3. Calculated STRESSES AND REPETITIONS TO
FAILURE FOR BEAMS TESTED UNDER VERTICAL
SHEAR TEST

Tack Coat	Beam Thickness, in.	Repeated Defl., in.	N_f 10^3	P lb	σT_1[1] psi	σT_2[2] psi	τ_1[3] psi	τ_2[4] psi
			Temperature of 77°F (25°C)					
RC-250	2	0.010	37.1	28.2	34.9	33.7	8.1	19.4
		0.035	0.471	82.0	101.	98.0	23.6	56.3
	4	0.010	5590	33.4	11.4	19.7	1.9	8.8
		0.035	0.104	94.8	32.3	55.7	5.3	25.0
A-R 0.5	2	0.010	0.711	28.2	30.7	10.2	2.6	2.1
		0.035	0.410	82.0	89.3	29.7	7.7	6.2
A-R 0.6	2	0.010	95.8	28.2	30.5	9.6	2.6	1.8
		0.035	0.664	82.0	88.6	27.9	7.4	5.2
	4	0.010	708	33.4	10.5	7.8	1.4	0.6
		0.035	4.09	94.8	29.8	22.3	4.0	1.7
A-R 0.7	2	0.010	52.7	28.2	30.2	9.1	2.5	1.6
		0.035	0.810	82.0	87.8	26.5	7.2	4.6
			Temperature of 40°F (4°C)					
RC-250	2	0.010	6066	75	92.8	89.6	21.6	51.5
		0.035	0.109	193	23.9	231	55.6	133
A-R 0.6	2	0.010	296	75	81.0	25.5	6.8	4.8
		0.035	0.676	193	208	65.6	17.5	12.3

1. Total tensile stress in the asphaltic beam at the joint.
2. Tensile stress in the tack coat at the joint
3. Horizontal shear stress in the asphaltic beam at the joint.
4. Horizontal shear stress in the tack coat at the joint.

Note: The stresses shown above were calculated assuming the following
elastic properties for the materials in the beams.

Asphaltic Concrete $E = 2 \times 10^5$ psi and $\nu = 0.35$
Tack Coat $E = 2 \times 10^3$ psi and $\nu = 0.45$
Aluminum $E = 1 \times 10^{11}$ psi and $\nu = 0.33$

A plot of log tensile stress-log repetition is shown for asphaltic beams as well as for the corresponding tack coats in Figure 10. The figure shows a separation by beam size and by tack coat.

For tensile stresses in the beams it is noted that tack coat had no effect on the fatigue relationship for the 2-inch (51 mm) beams as has been noted earlier based on deflections. For the 4-inch (101 mm) beams relationship is not definitive.

The points for the 4-inch beams do not fall on the 2-inch beam line which is as it should be since the test specimens were not linear elastic materials and thus a transverse plane in the asphaltic beam before bending will not be a plane after bending.

In the elastic analysis of the composite beam the tack coat was assumed to act as a membrane, that is, it did not have bending stresses but axial ones. As a consequence the data points for tension in the tack coats seem to be greatly affected by type of tack coat and not largely affected by beam thickness.

A plot of points similar to that of Figure 10 is shown in Figure 11 for the maximum shear stress in the beams. The data points for shear stress in the tack coat are not shown since no significant relationship was obvious for this comparison. Figure 11 does show that points representing the 2 and 4-inch beams with all tack coats of A-R do have a locus about a straight line.

In general it appears that the fatigue life developed experimentally between deflection and number of repetitions to failure could be more generally represented with the calculated shear stress in the asphaltic beam and to a slightly lesser degree with the calculated tensile stress

Figure 10. Relationship between Repeated Tensile Stress and Number of Repetitions to Cause Failure in the Vertical Shear Test

37
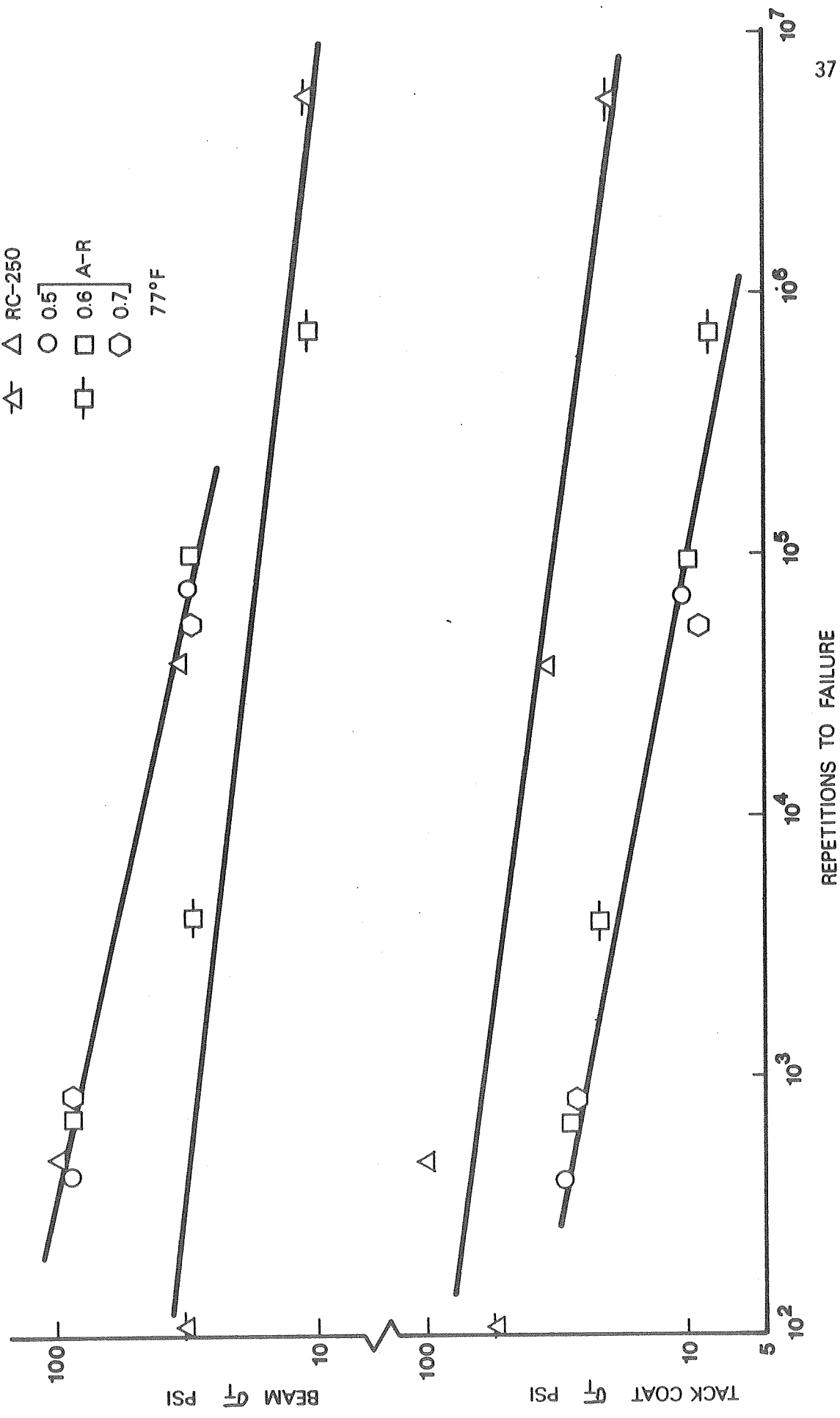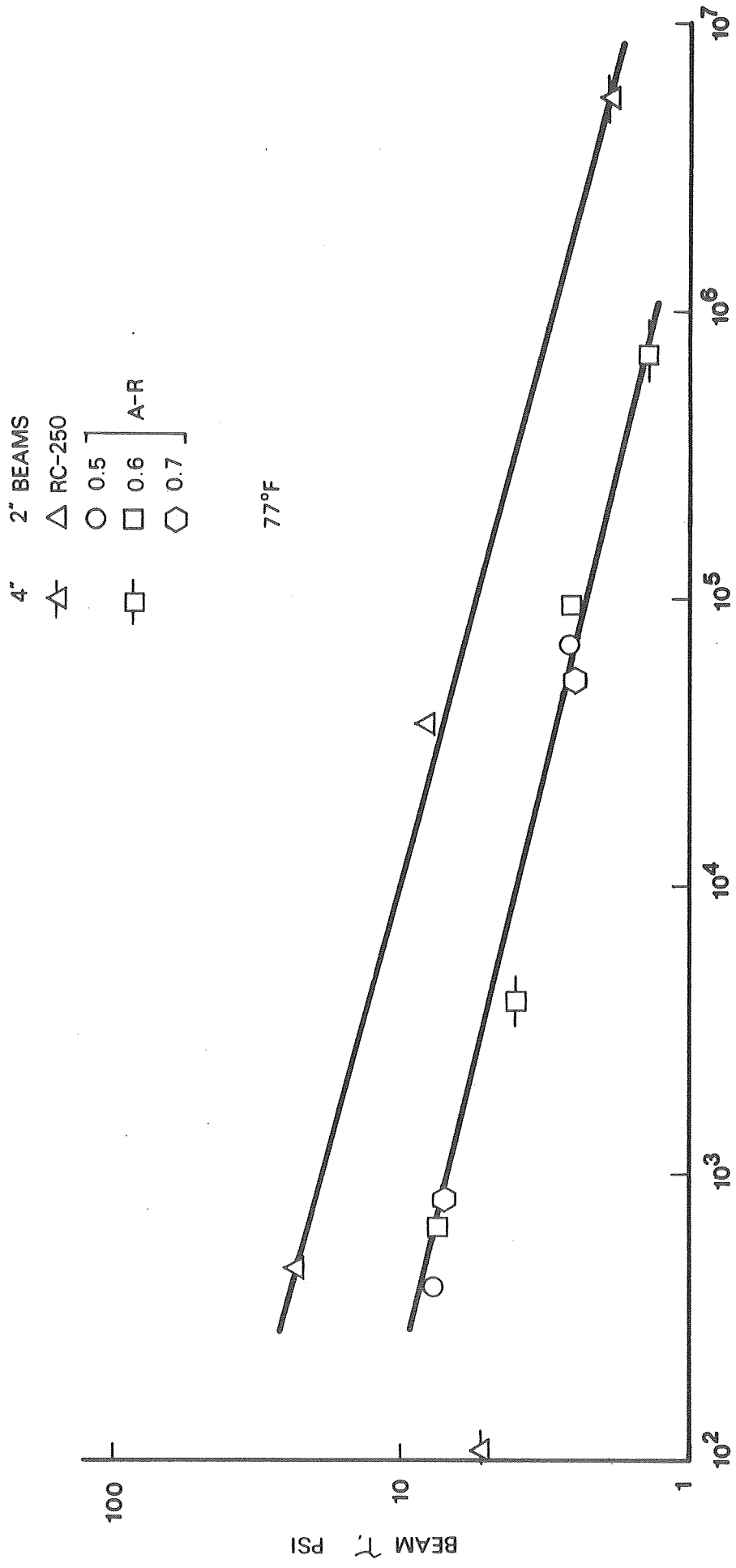
Figure 11. Relationship between Repeated Shear Stress and Number of Repetitions to Cause Failure in the Vertical Shear Test

38

in the tack coat. Of course, the calculated data are somewhat limited especially since only one set of elastic values for modulus of elasticity and Poisson's ratio was used for each material of the composite beam.

CONCLUSIONS

The work performed in this study was aimed at determining or developing test methods for characterizing asphalt-rubber for its performance as a strain attenuating material and pavement layer. The literature review and tests performed have been discussed with reference to the material, A-R, and its performance as a layer in a composite beam tested under simulated service conditions that result in reflection cracking.

Within the limits of the materials and scope of the study, the findings and conclusions are summarized as follows:

1. The swelling of the rubber particles by benzene (an aromatic compound) was primarily a physical effect.

2. The mixing and storage procedure used for A-R resulted in a constant material for storage time varying from 3 days to 3 weeks.

3. The falling coaxial cylinder viscometer built to make viscosity measurements of the A-R and base asphalt produced acceptable repeatability of measurements.

4. The viscosity of the A-R was about 200 times greater than the base asphalt at $140^{\circ}F$ ($60^{\circ}C$) but about 6 times smaller than the asphalt at $32^{\circ}F$ ($0^{\circ}C$).

5. The variations of the ductility test performed indicated that the A-R's values were not significantly affected by the temperature changes from $77-33^{\circ}F$ ($25-0.5^{\circ}C$).

40

6. The literature survey and the ductility test results suggest that the rubber fines act as elastic aggregate in the A-R blend. On this basis it would be anticipated that the A-R may have lower values of cohesion and adhesion than the straight asphalt.

7. The test results from the horizontal shear test (simulating thermal stresses) indicate that the A-R will serve quite effectively as a strain attenuating layer and that heavier applications of A-R are necessary as the thickness of the overlay increases. Data were not obtained to establish a safe maximum thickness of A-R for use as a SAL.

8. The results from the vertical shear test (simulating repeated wheel load shear) suggest that the principal benefits of the A-R serving as a SAL came from maintaining its pliability at lower temperatures. The data for the $77^{o}F$ ($25^{o}C$) did not show significantly difference in performance for the tack coats (SAL) of RC-250 and the A-R.

9. The calculation for stresses in the composite beam based on linear elastic theory indicated that tensile stress in the SAL and also the shearing stress in the asphaltic beam (overlay) could represent deflection in the repeated deflection versus number of repetitions to cause failure (δ-N) fatigue relationship found with the vertical shear test.

10. It is believed that the equipment developed for the two test procedures for evaluation of SAL proved to yield repeatable results. However, an expanded laboratory testing program and field verification is necessary.

11. As with the new testing procedures developed, the mathematical analysis for stresses in the composite beam should be expanded for numerically detailing the value of stresses throughout the composite beam.

Recommendation

The results of this research have yielded positive and directional expressions for the A-R to serve as an effective strain attenuating layer. It is recommended that a designed field experiment be conducted in which the principal variables be (a) amount of A-R, (b) the thickness of overlay, and (c) stiffness of the pavement system.

Implementation Statement

This study is concerned with laboratory testing of an asphalt and rubber (A-R) mixture with special emphasis towards its use to minimize reflective cracking. Two special tests were developed to compare A-R and RC-250 as tack coats and acting as strain attenuating layers (horizontal shear test); a repeating beam deflection test (vertical shear test).

Both test procedures will undergo further testing and evaluation.

ACKNOWLEDGEMENT

REFERENCES

1. McDonald, Charles H., "A New Patching Material for Pavement Failures," HRR 146, Highway Research Board, 1966.

2. Olsen, Robert E., "Rubber-Asphalt Binder for Seal Coat Construction," Implementation Package 73-1, U.S. Federal Highway Administration, 1973.

3. Morris, Gene R. and McDonald, Charles H., "Asphalt-Rubber Stress Absorbing Membranes," a report presented at the Annual Meeting of the Transportation Research Board, 1976.

4. "Bituminous Materials in Road Construction, Roads Research Laboratory, Her Majesty's Stationery Office, London, 1962.

5. Clemmer, H. F. and Smith, N. G., "Rubber in Bituminous Pavements," Technical Bulletin No. 194, ARBA, 1953.

6. Gregg, L. E., "Additional Observations on the Use of Rubber in Bituminous Paving Mixtures," Technical Bulletin No. 194, ARBA, 1953.

7. Welborn, J. York, and Babashak, John F., Jr., "A New Rubberized Asphalt for Roads," Proceedings, (HW2) ASCE, 1958.

8. Endres, H.A., "Latest Developments in Rubberized Asphalt," A paper presented at the Fourth Annual Highway Conference at the University of the Pacific, Stockton, California, 1961.

9. LaGrone, B. D. and Huff, B. J., "Use of Waste Rubber in Asphalt Paving," a paper prepared for presentation at the Colorado State University Asphalt Paving Seminar, Fort Collins, Colorado, 1973.

10. Oliver, J. W. H., "A Critical Review of the Use of Rubbers and Polymers in Bitumen Bound Paving Materials," Internal Report AIR 1037-1, Australian Road Research Board, 1977.

11. Green, E. L. and Tolonen, William J., "The Chemical and Physical Properties of Asphalt-Rubber Mixtures," Report ADOT-RS-14(162), Arizona Department of Transportation, 1977.

12. Frobel, R. K., Jimenez, R. A. and Cluff, C. B., "Laboratory and Field Development of Asphalt-Rubber for Use as a Waterproof Membrane," Report ADOT-RS-14(167), Arizona Department of Transportation, 1977.

13. Kalash, R. H., "Asphalt-Rubber Mixtures for Seepage Control," M. S. Thesis, University of Arizona, 1977.

14. Supplemental to Standard Specifications for Road and Bridge Construction, Arizona Department of Transportation, 1975.

15. Jimenez, R. A., "Structural Design of Asphalt Pavements - II," Report ADOT-RS-13-(142), Arizona Department of Transportation, 1975.

16. Traxler, R. N. and Schweyer, H. E., "Measurement of High Viscosity-- A Rapid Method," Proceedings, ASTM, Vol. 36, Part III, 1936.

17. McCullagh, Frank R., "Reflection Cracking of Bituminous Overlays on Rigid Pavements," Special Report 16, New York State Department of Transportation, 1973.

18. McGhee, K. H., "Efforts to Reduce Reflective Cracking of Bituminous Concrete Overlays of Portland Cement Concrete Pavements," Report VHTRC-R20, Virginia Highway and Transportation Council, 1975.

APPENDICES

Appendix A - Test Data

Appendix B - Blending of Asphalt and Rubber

Appendix C - Viscometer Test Procedure

Appendix D - Compaction of Beams

Appendix E - Horizontal Shear Test

Appendix F - Vertical Shear Test

Appendix G - Bending of a Composite Beam

TABLE 1A. CHARACTERISTICS OF THE ASPHALT CEMENT
(ADOT Lab Test No. 76-40149)

	ADOT Specification	Test Value
Flash Point, P.M., °F, min.	400	455
Solubility in trichloroethylene, %, min.	99	-
Penetration, 100 g., 5 sec., 77°F		120
Viscosity, abs., 140°F, P.		744
Viscosity, in., 275°F, cs.		167
Test on 75 min., RTFC residue		
Viscosity, abs., 140°F, p.	750-1250	1410
Viscosity, kin., 275°F, cs., min.	140	-
Penetration, 100 g., 5 sec., 77°F, min.	65	78
Ductility, 77°F, cm., min.	100	-

TABLE 2A.   GRADATION OF RUBBER FINES   (TP 044)*

Sieve no.	8	16	25	30	50	100
Opening, in.	0.094	0.047		0.023	0.012	0.006
			Total Percent Passing			
ADOT specs., dry	100	95	10	--	--	--
Tested						
Air dry	100	99		20	2	0
Soaked in benzene for 2 hours and then dried at 140°F	100	99		22	1	0
Soaked in benzene for 24 hours and then dried at 140°F	100	99		29	1	0

---

* Overflex from Atlos Rubber Inc., Los Angeles, California

TABLE 3A. CHARACTERISTICS OF 3/4" TANNER ASPHALTIC
CONCRETE

	Density pcf	Hveem Stab.,%	Cohesiometer Value	Double Punch Tension,77°F,psi
4"D by Cal. Kndg[1] Compactor	143.0	19.0	320.0	--
4"D by Vib. Kndg[2] Compactor	145.0	50.0	275.0	124.0
5"x12"x2½" Beam 1 layer VKC[2]	142.5			
4"D Core	142.0	--	--	82.0
5"x12"x4" Beam 1 layer VKC[2]	139.5			
5"x12"x4" Beam 2 layers VKC[2]	140.5			

[1]California kneading compactor
[2]Vibratory kneading compactor

TABLE 4A.   CHARACTERISTICS OF 1/2" TANNER ASPHALTIC
CONCRETE

	Density pcf	Hveem Stab.,%	Cohesiometer Value	Double Punch Tension,77°F,psi
4"D by Cal. Kndg Compactor	143.0	28.0	345.0	--
4"D by Vib. Kndg Compactor	141.0	--	--	101.0
5"x12"x2½" beam 1 layer VKC	139.0			
4"D Core	139.0			92.0
Beams after Vertical Shear Test 2" and 0.7 A-R	138.0			
	140.0			
4" and 0.6 A-R	139.5			
	139.5			

TABLE 5A.   VISCOSITIES OF ASPHALT CEMENT AND
ASPHALT-RUBBER BY FALLING COAXIAL CYLINDER

$$S_S = IS_R^{\,c}$$

Temp. $^\circ F(C^\circ)$	Test No.	I $10^5 dyne/cm^2$	c	n	R^2	$\eta_{0.05}$ sec^{-1} 10^6 poise
		Asphalt Cement AR-1000				
	1	158.05	1.143	4	0.998	10.30
	2	83.11	1.019	4	0.992	7.85
59(15)	Comb.	102.55	1.062	8	0.978	8.52
	3	120.53	1.071	4	0.992	9.60
	4	80.43	1.001	4	0.992	8.02
59(15)	Comb.	67.32	0.974	8	0.990	7.28
	1	4.00	0.912	4	0.998	0.521
	2	4.09	0.915	4	0.998	0.324
77(25)	Comb.	3.81	0.902	8	0.998	0.511
	1	0.97	1.253	4	0.999	0.045
	2	1.12	1.284	4	0.999	0.048
95(35)	Comb.	1.23	1.323	8	0.990	0.047
	1	1.31	1.361	4	0.994	0.044
	2	1.56	1.417	4	0.994	0.046
95(35)	Comb.	1.35	1.366	8	0.994	0.045

TABLE 5A (cont'd)

$$S_S = IS_R{}^c$$

Temp. $^oF(^oC)$	Test No.	I $10^5 dyne/cm^2$	c	n	R^2	$\eta_{0.05} sec^{-1}$ 10^6 poise

Asphalt-Rubber

	1	13.45	0.522	4	0.978	5.631
	2	11.41	0.480	4	0.970	5.418
57(14)	Comb.	13.13	0.503	8	0.939	5.819
	1	5.03	0.618	4	0.861	1.580
	2	25.22	0.924	4	0.897	3.167
77(25)	Comb.	8.78	0.722	8	0.854	2.019
	3	3.06	0.407	4	0.504	1.808
	4	12.28	0.659	4	0.992	3.410
77(25)	Comb.	8.48	0.584	8	0.774	2.949
	1	3.25	0.938	4	0.974	0.391
	2	1.65	1.316	4	0.931	0.064
104(40)	Comb.	3.95	1.004	8	0.861	0.390
	3	0.73	0.605	4	0.998	0.238
	4	1.01	0.658	4	0.999	0.281
104(40)	Comb.	0.74	0.605	8	0.916	0.242

TABLE 6A. DUCTILITY VALUES FOR ASPHALT CEMENT
AND ASPHALT-RUBBER

Extension Speed cm/min.	Asphalt Cement Test Temp. ^{O}F			Asphalt-Rubber Test Temp. ^{O}F		
	77	55	33	77	55	33
5	150$^+$	150$^+$	0	22	29	22
11	150$^+$	150$^+$	0	25	27	16
19	150$^+$	150$^+$	0	22	24	19

77^OF = 25^OC
55^OF = 12.7^OC
33^OF = 0.5^OC

TABLE 7A.   RESULTS FROM THE HORIZONTAL SHEAR TEST
FOR THE RC-250 TACK COAT (0.05g.s.y
and 3/4"-ASPHALTIC CONCRETE).

Speed, in/min.	0.05		0.10		0.20	
Thickness, in.	2	4	2	4	2	4
Max. Load, lb.	65	115	175	210	300	470
	80	112	160	210	280	480
Avg.	72	113	167	210	290	475
Slip @ Max. Load 10^{-4} in.	210	180	130	110	50	35
	150	60	160	80	56	65
Avg.	180	120	145	145	53	50

TABLE 8A. RESULTS FROM THE HORIZONTAL SHEAR TESTS
FOR THE ASPHALT-RUBBER TACK COAT
(0.5 to 0.7g.s.y and 3/4"-ASPHALTIC CONCRETE).

Speed, in/min.	0.05		0.10		0.20	
Thickness, in.	2	4	2	4	2	4

0.5 gal. per sq. yd.

Max. Load, lb.	147	170	188	240	165	220
	183	195	218	218	240	255
Avg.	165	183	203	229	203	237
Slip @ Max. Load	280	150	360	450	750	350
10^{-4} in.	200	300	---	280	700	350
Avg.	240	225	360	365	725	350
Slip at Rupture	650	500	620	530	1400	900
10^{-4} in.	800	800	---	315	1350	650
Avg.	720	650	620	423	1375	775
Load at Slip	133	145	188	240	160	175
Rupture, lb.	140	165	212	215	240	235
Avg.	136	155	200	227	200	205

TABLE 8A. (cont'd).

Speed, in/min.	0.05		0.10		0.20	
Thickness, in.	2	4	2	4	2	4

<u>0.6 gal. per sq. yd.</u>

	2	4	2	4	2	4
Max. Load, lb.	125	135	130	177	180	230
	102	107	180	170	185	270
Avg.	113	122	155	173	183	250
Slip @ Max. Load 10^{-4} in.	610	410	740	700	950	800
	860	420	470	840	1000	300
Avg.	735	405	605	770	975	550
Slip at Rupture 10^{-4} in.						---
						880
Avg.	NA	NA	NA	NA	NA	880
Load at slip Rupture, lb.						---
						220
Avg.	NA	NA	NA	NA	NA	220

TABLE 8A. (cont'd.).

Speed in./min. Thickness, in.	0.05		0.10		0.20	
	2	4	2	4	2	4

<u>0.7 gal. per sq. yd.</u>

	2	4	2	4	2	4
Max. Load, lb.	95	120	90	205	160	170
	110	140	130	---	160	---
Avg.	103	130	110	205	160	170
Slip @ Max. Load 10^{-4} in.	900	720	500	400	1200	950
	1000	480	1100	---	1200	---
Avg.	950	650	800	400	1200	950
Slip at Rupture 10^{-4} in.	1300	1700	900	1200	2400	2000
	1200	1200	3000	----	2100	----
Avg.	1250	1450	1850	1200	2250	2000
Load at Slip Rupture lb.	95	115	85	180	155	160
	110	100	125	---	160	---
Avg.	102	107	105	180	157	160

TABLE 9A. RESULTS FROM THE REPEATED VERTICAL SHEAR
TEST FOR THE RC-250 TACK COAT
(0.05g.s.y. and 1/2"-ASPHALTIC CONCRETE)

Beam Thickness in.	2"				4"	
Test Temp. °C	25^{0}		4^{0}		25^{0}	
	Rep. δ	N_f	Rep. δ	N_f	Rep. δ	N_f
	10^{-3} in.	10^{3}	10^{-3} in.	10^{3}	10^{-3} in.	10^{3}
	5	$2,000^{+}$	20	5.0	14	300
	10	32.0	20	155	15	125
	11	35.0	23	2.2	16	52
	18	4.0	25	1.2	17	110
	20	3.0	27	2.2	19	16
	28	0.8	33	0.3	20	30
	35	0.7	42	0.02	20	17
	43	0.2			21	11

TABLE 10A. RESULTS FROM THE REPEATED VERTICAL SHEAR TEST FOR THE ASPHALT-RUBBER TACK COAT (0.50-0.70 g.s.y. and 1/2"- ASPHALTIC CONCRETE)

Test Temperature °C	25°								4°	
Beam Thickness, in.	2		2		2		4		2	
Amount of Tack, g.s.y.	0.50		0.60		0.70		0.60		0.60	
	Rep. δ 10^{-3} in.	N_f 10^{-3}	Rep. δ 10^{-3} in.	N_f 10^{-3}	Rep. δ 10^{-3} in.	N_f 10^{-3}	Rep. δ 10^{-3} in.	N_f 10^{-3}	Rep. δ 10^{-3} in.	N_f 10^{-3}
	6 7	530.0 301.6	7 12	509.0 35.8	4 10 11	2,000$^+$ 55.0 42.0	13 15	222 130	10 12	350.0 90.0
	13 25	26.0 2.0	13 20 21	32.0 4.6 6.0	15 17 20	9.0 9.0 6.0	16 19	130 45	16 20 23	28.0 6.2 7.1
	40 45	0.5 0.2	34 45	0.7 0.3	28 30	1.9 1.0	30 33	8 4.3	26 26 37	2.0 3.5 0.5

APPENDIX B

Procedure Used for Blending Asphalt and Rubber

1. Equipment

    a. 1-quart size stainless steel sauce pan, 6-inch diameter by
        3.5-inch deep (152Dx89Hmm).

    b. 5-inch diameter (127Dmm) ring gas burner.

    c. Electric motor mixer with powerstat and a 3-inch (76mm) - 3
        bladed propeller.

    d. Ring stand, 5-inch (127mm) ring, and asbestos wire gauge.

    e. Thermometer 30° to 760^OF (-1 to 404^OC), 8F.

    f. Watch or clock.

2. Asphalt sample of 750± grams in sauce pan and 250± grams of rubber
    in a container; both at ambient temperature. The rubber to have
    been dried in a 140^OF (60^OC) oven for 15 hours and stored in a
    sealed container.

3. Assemble as shown in photograph of Figure B1.

4. Melt asphalt to temperature of 120-160°F (49-71°C) and position
    thermometer and mixer in the hot asphalt. Rotate the propeller so
    that there is no splashing and a vortex is formed between the
    center and side of pan.

5. Raise the temperature of the asphalt at a rate of 10°-12^OF (6-8°C)
    per minute to reach 375°F (191°C). Now add the rubber to the
    asphalt at the edge of the vortex in small increments so that the

60

total amount is introduced in five minutes. It will be necessary to increase the power of the stirrer as the viscosity of the mixture increases. Also the colder rubber will reduce the temperature and adjustment to the gas flow is necessary.

6. Continue the mixing for 30 minutes after all of the rubber has been added. Adjustment to the stirrer and burner are necessary as viscosity and temperature changes occur. Try to hold the mixing temperature at $375^{\circ}F$ ($191^{\circ}C$). The temperature may drop to $355^{\circ}F$ ($179^{\circ}C$) at the beginning and may rise to $395^{\circ}F$ ($202^{\circ}C$). Also it may be necessary to cut the gas off completely. Additional stirring with a 6-inch (152 mm) spatula is desirable. The thermometer reading is affected by presence or absence of rubber around its bulb.

7. After the final 30 minutes of mixing, place weighed amounts of the hot asphalt-rubber into lidded metal containers for storage. The amounts of asphalt-rubber vary from 30 to 125 grams for making specimens to be tested for viscosity or in the asphaltic-aluminum beam set-up.
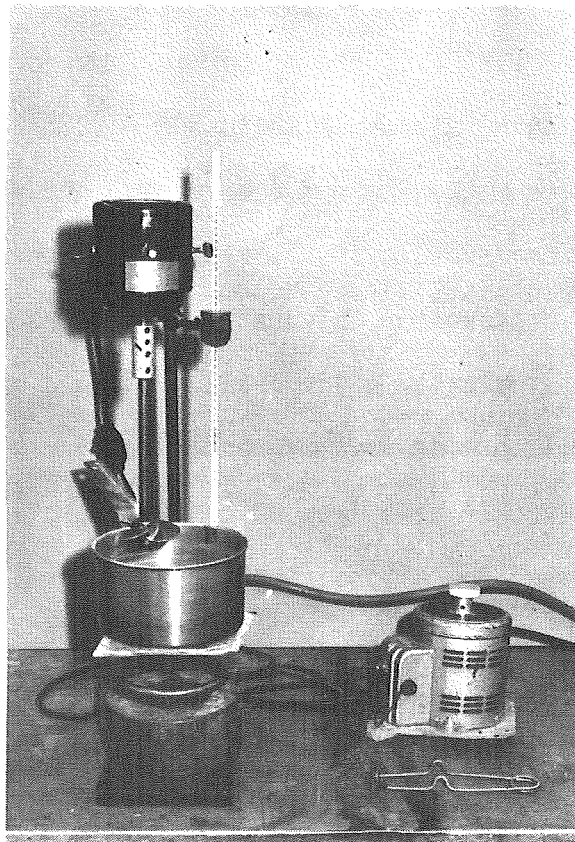
Figure 1B. Set-up for Blending Asphalt and Rubber

APPENDIX C

Procedure Used for the Falling Coaxial Cylinder Viscometer

1. Equipment

    a. Various cylinders and pistons for the viscometer meeting the geometry requirement that the ratio of annulus width/length is less than 0.5.

    b. Water bath with temperature control, stirrer, and thermometer meeting ASTM requirments.

    c. Cathetometer and extensometer dial gauge with 0.001-inch (0.03mm) divisions.

    d. Stop watches.

    e. Silicone lubricant.

2. Sample preparation

    a. Lightly coat a 4"x4"x1/4" (102x102x6mm) glass plate with the silicone lubricant, also the upper portion of the aluminum piston and the inside of the aluminum centering ring.

    b. Asphalt is heated to a fluid condition and poured into the annular space of the cylinder-piston assembly resting on the glass plate. Overfill the viscometer so that upon cooling there is an excess of asphalt to be trimmed. Recenter the piston with the centering ring.

    b'. Asphalt-rubber from storage, the cylinder, and the piston of a viscometer-set are heated to about 250°F (121°C) in an oven. The heated cylinder only is placed on a silicone coated glass

63

plate and then filled to 0.6 of the length with the heated asphalt-rubber. The hot piston is then forced through the hot asphalt-rubber until it makes contact with the glass plate and making sure that there is a slight excess of asphalt-rubber. The centering ring is now placed on the viscometer. Check the bottom of the viscometer for air voids.

c. Allow the assembly of b or b' to cool at room temperature until firm and then trim the excess asphalt with a hot spatula. The sample is kept at room temperature after pouring or packing for a period of 60 to 90 minutes.

d. The assembly on the glass plate is then placed in the water bath at the desired test temperature for a period of 60 to 90 minutes prior to testing.

e. Testing should be completed within 3 1/2 hours from casting of the sample.

3. Testing

a. Place viscometer support in the water bath and adjust legs so that the support is level and the water level will be at least 1.5 inches (38 mm) above the sample. The depth to the viscometer support shoulder must be determined to compute the buoyant force.

b. Set up the cathetometer or extensometer gage bar. The cathetometer is used when the spring-force of the extensometer causes a significant amount to the shearing stress. The cathetometer telescope is sighted on a mark on the piston. The extensometer tip is to bear on the top of the piston of the viscometer.

c. Remove the centering ring and place the viscometer on the depressed shoulder of the support stand.

d. Determine the time required for the piston to drop a predetermined distance for at least four consecutive periods. The total distance of piston fall should not exceed one-tenth (0.1) the length of the sample and each time period should be not less than about ten seconds.

e. Repeat the time measurements using at least four different weights on the piston. After each run of four time measurements, the piston is returned to the original base position by pressing the viscometer assembly on the silicone coated glass plate. Also, after each run the viscometer is kept in the water bath for a minimum recovery period of ten minutes. During the recovery period a second sample may be tested.

4. Calculations

a. The velocity of the piston for determination of the shear rate is determined from a plot of cumulative displacement (the ordinate) versus cumulative time (the abscissa). The velocity is determined from the linear portion of displacement-time curve and reported in units of centimeters per second.

b. The shear rate is the velocity gradient within the annulus and calculated by dividing the velocity by the width of the annulus. The shear rate (S_R) has units of reciprocal second (sec^{-1}).

c. The shear stress is the vertical stress on the interface of piston and asphalt and is expressed as follows:

$$S_S = F_{eff} \frac{g}{2\pi rL}$$

Where: F_{eff} is the effective force in g (total piston weight

minus the bouyant force)

g is gravity, 980 cm/sec^2

r is the radius of the piston, cm

L is the length of the annulus, cm

S_S is the shear stress, dyne per cm^2

d.   Plot the calculated values on log-log paper with shear stress as ordinate and shear rate as abscissa. The "best" straight line is drawn by eye through the data points.

e.   Viscosity is defined as the slope of the S_S vs S_R (Cartesian coordinates) curve or simply

$$\eta \ (viscosity) = \frac{S_S}{S_R}$$

Since the S_S vs S_R curve is not linear for most asphalt, it has been customary to evaluate viscosity at a shear rate of 5×10^{-2} sec^{-1}. To determine viscosity, find the shear stress corresponding to the reference shear rate of 5×10^{-2} sec^{-1} from the log-log graph and then divide by the reference shear rate. The unit of viscosity will then be $\frac{dyne\text{-}sec}{cm^2}$ or poise.
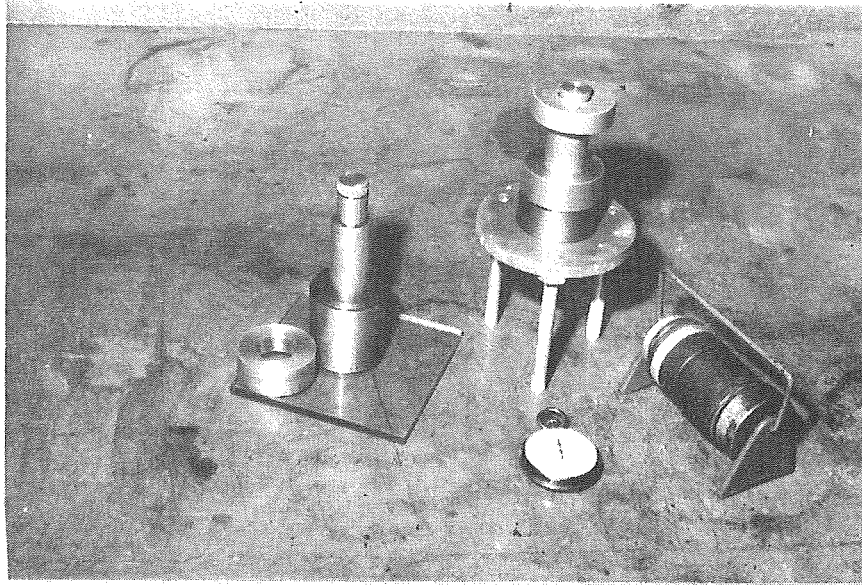
a. Coaxial Cylinder Viscometers
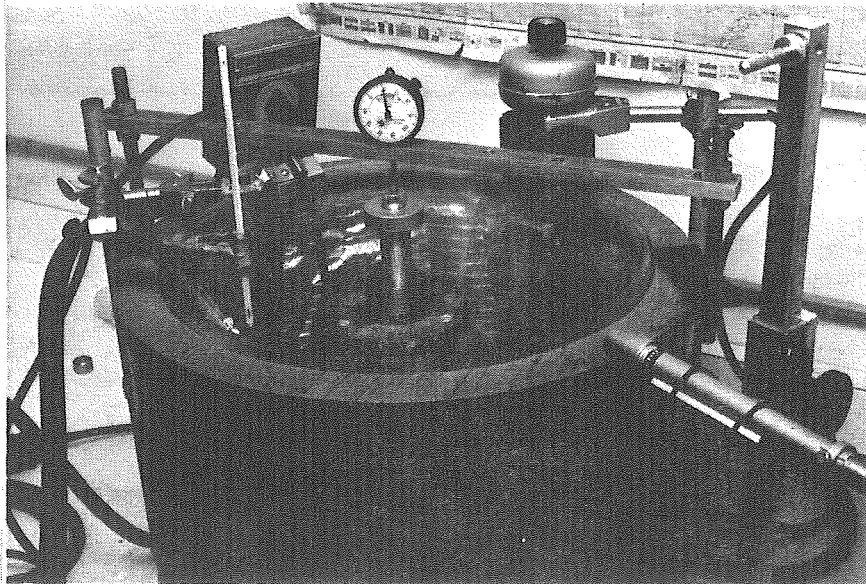
b. Test Set-up for Coaxial Cylinder Viscometer

Figure 1C. Photographs of Coaxial Cylinder Viscometers

APPENDIX D

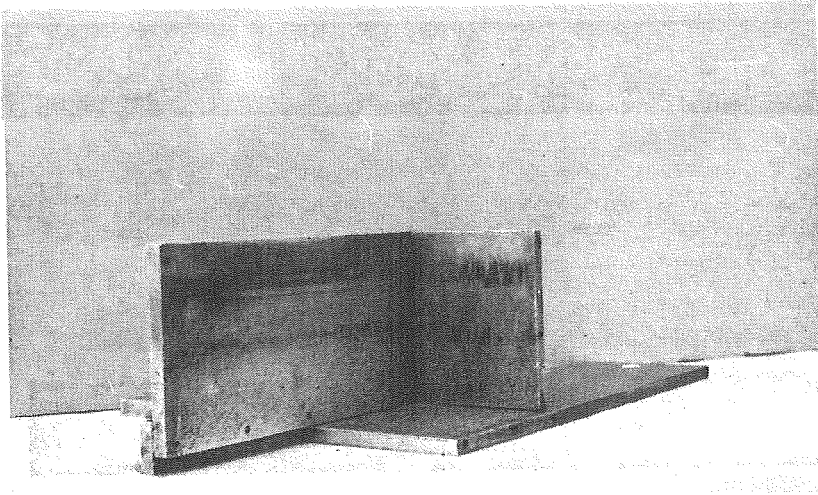Procedure Used for Compaction of Asphaltic--Aluminum Beams

Note: A supply of asphaltic concrete has been obtained and is stored
in sealed 5-gallon (19 1.) cans. A record is kept of the amount of
mixture remaining in each can.

    a. Place sealed can of asphaltic concrete in a 180°F (82°C) oven
       for about 1½ - 2 hours so it becomes soft enough to sample.

    b. While the mixture is in the oven (item a), assemble the
       aluminum mold-beam unit. Asphaltic portion of the beam will
       be 5 inches (127mm) wide and 12 inches (305mm) long. After
       assembly, heat the unit on a large hot plate or oven and then
       spread the hot asphalt-rubber tack coat on the inside base of
       the mold at the predetermined rate. The cold asphalt-rubber
       is in metal cans containing a slight excess of the amounts
       required to yield the spread rates of 0.5, 0.6, and 0.7 gallons
       per square yard (2.3, 2.7, and 3.1 liters per square meter).
       If the tack coat is to be RC-250, it is applied at least 24
       hours prior to making the beam and the cutter stock is allowed
       to evaporate at room temperature. Do not accelerate the loss
       of cutter stock with the use of heat since the tack coat will
   draw away from the sides of the mold and also leave bare spots.

c. When the asphaltic concrete of item a is soft enough, withdraw the can and scoop out 2,150 grams of mixture for each 1 inch of beam thickness desired. The sample in a metal pan is then placed into a 250°F (121°C) oven for about 2 hours or until the mixture comes to the oven temperature. A dial thermometer is inserted into the loose mixture.

d. When the mixture is at 250°F (121°C), place it into the cold prepared mold. The maximum thickness to be compacted at one time is 2 inches (51mm). The loose mixture is rodded 25 times with a 3/8-inch (9.5mm) diameter by 18-inch (457mm) long bullet-nosed steel bar and then level the surface with the I-beam ram by pushing or rocking manually. Then place a 5 x 12-inch (127x305mm) piece of heavy paper on top of the mixture, and then place the 0.090 inch (2.3mm) thick steel plate (5x12 inches) in the mold and on the paper.

e. The beam will be compacted using vibratory forces and the vibratory kneading compactor. The procedure includes the following:

1. frequency of 1200 rpm

2. 4-inch by 5-inch (101 x 127mm) foot

3. no tilt of turntable

4. no rotation of turntable

5. attachment for guiding the beam-mold assembly

Densification is obtained by compacting for four minutes for each inch (25.4mm) of beam thickness while the mold is being moved back and forth 8 inches (203mm) at a rate of 5 cycles per minute. Attention should be paid to compact the beam

evenly. When beams thicker than 2 inches (51mm) are desired, compact the first layer equal to one-half of the total thickness and then score the surface before placing the additional mixture for the next layer. The scoring is to minimize having a plane of weakness.

f. After vibratory compaction, remove the beam-mold assembly and place it on the platen of the Riehle testing machine. The swivel head of the testing machine is fixed with the aluminum plate to keep the head surface parallel to the platen. Place the I-beam ram in the mold and then apply a total load of 18,000 pounds (8,165 kilogram) which corresponds to 300 psi (21.1 kg/cm^2) and hold it for 2 minutes and then remove the load. This loading is to produce a smooth and parallel surface on the top of the beam; no compaction is effected.

g. After the leveling load has been applied, allow the assembly to set for one day at room temperature and then remove the side and end mold plates. Now, immediately attach the holding bars to the aluminum portions of the beam while making sure that the two aluminum plates lie on a plate.

h. Allow the asphaltic-aluminum beam to cure for at least 3 days at $77^{o}F$ ($25^{o}C$) prior to testing.

a. Partial Mold for Asphaltic-Aluminum Beam
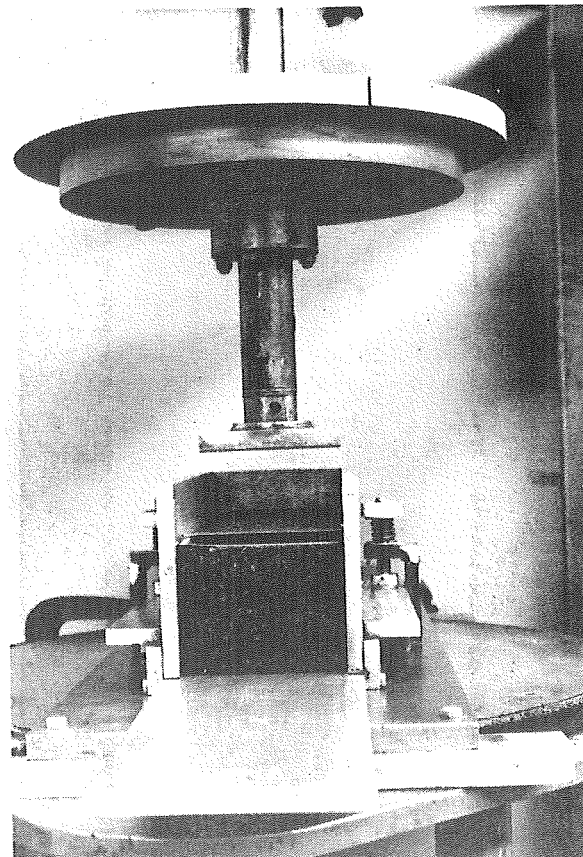
b. Vibratory-kneading Compaction
of Beam

Figure 1D. Set-up for Making Asphaltic-Aluminum Beam

APPENDIX E

Procedure Used for the Horizontal Shear Test

Note: The asphaltic-aluminum beam has been stored in a 77°F (25°C)
room. Determine and record the thickness of the asphaltic portion of the
beam. Testing will be done at ambient temperature on the Riehle test-
ing machine; however, as much as possible of the set-up will be done
in the 77°F (25°C) room.

   a. Lay the beam assembly on its side on a level surface and remove
       the exposed holding bar. Rotate the assembly about its long
       axis and remove the second holding bar. At all times be
       extremely careful not to cause displacement of the aluminum
       plates relative to each other or the asphaltic beam.

   b. While the assembly is on its side, lift it gently and slide
       the clamping-plate assembly onto the beam and spanning the joint;
       then uniformly finger-tighten the wing-nuts without deforming
       the beam.

   c. Lay the assembly back upright (on the wide side) and attach
       the gauge bracket mount having an extensometer with 0.0001
       inch (0.002mm) graduations.

   d. Place the 3/4 inch (19mm) diameter rods through the holes of
       the two crossheads of the testing machine. Now slip the beam
       onto the bar, the top one first and then the bottom one. The
       end with the extensometer is the lower one.

72

e. Place the support base of a second extensometer dial gage on the testing machine platen to measure the downward movement of the lower crosshead. This second gage has graduations of 0.001 inch (0.025mm).

f. Zero both dial gages; tare and zero the testing machine. Set the load scale on 0-1200 pound (0-54 kg).

g. Carefully loosen the clamping plates and slide them upward and past the joint of the aluminum plates. Now finger-tighten the wing-nuts. This position of the clamping plates is to force relative motion to occur on the lower half of the beam at the asphalt-aluminum interface where this motion is measured with the 1/1000 inch (0.002mm) gage.

h. Set the speed control dial at the desired crosshead displacement rate and then apply tensile load (downward movement). Record load and relative displacement (slip) of aluminum plate to asphalt at selected interval of crosshead displacement: these intervals depend on the crosshead speed as shown below:

Crosshead Speed inch/minute	Crosshead Displacement inch
0.05	0.005
0.10	0.010
0.20	0.020

Usually three persons will be required to call and record readings. Loading is continued past the maximum force until the slip rate at the interface of the beam equals the crosshead speed. Of course, the test ends if the asphaltic beam fractures.

i. Reverse the direction of the crosshead until the beam is free for removal and being careful not to jam or apply compressive loads to the assembly.

j. After the aluminum plates have been removed, warm them in a $250^{\circ}F$ ($121^{\circ}C$) oven to facilitate the removal of the asphaltic beam and for cleaning the plates.
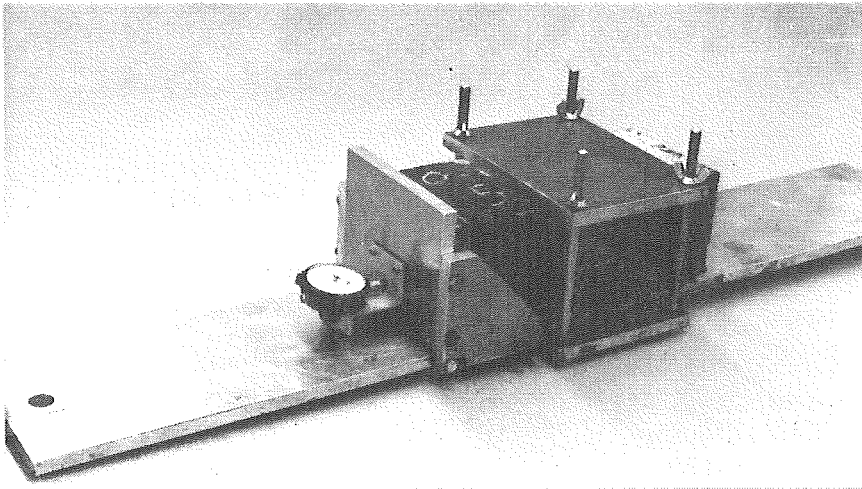
a. Beam Assembled for Horizontal Shear Test
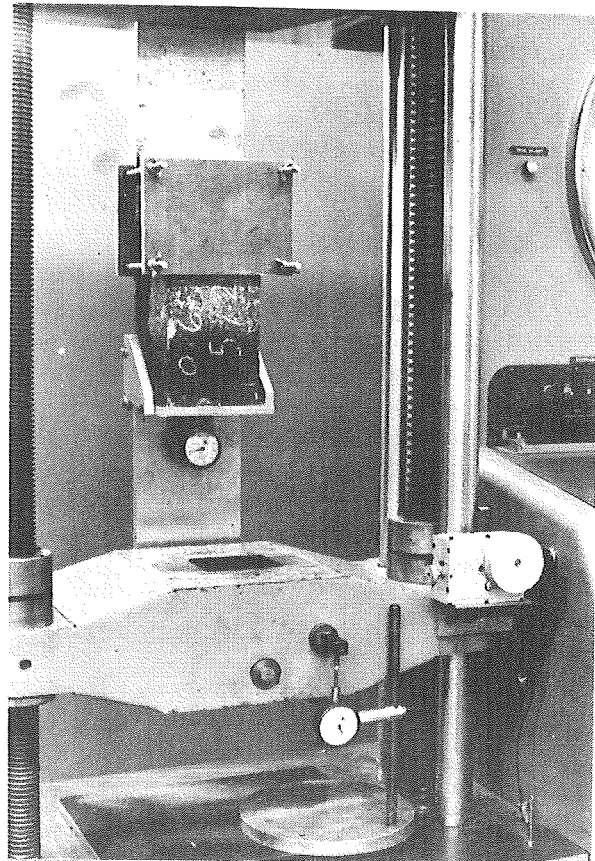
b. Horizontal Shear Test Set-up

Figure 1E. Photographs of the Horizontal Shear Test

APPENDIX F

Procedure Used for the Vertical Shear Test

Note: The asphaltic-aluminum beam has been stored in a controlled temperature room. Determine and record the thickness of the asphaltic portion of the beam. The testing device which consists basically of a variable eccentricity cam and four supports for the beam is in the controlled temperature room.

a. Set the cam eccentricity desired by rotating the outer cylinder and measuring the eccentricity with an extensometer gauge.

b. Place the beam assembly on the supports with the identification writing facing forward. Position the plates so that the joint is one-half inch (12.5mm) to the left of the drive shaft axis.

c. Remove the holding bars. Place the top extensometer dial over the top of the beam in line with the drive shaft and zero the indicator. Secure the beam assembly by tightening the clamping bars to the supports in the following sequence:

1. snug bar #1 (inside right)

2. snug bar #3 (inside left)

3. tighten bar #1

4. tighten bar #3

5. repeat the above sequence (1-4) for bars #2 and #4

The beam assembly has been secured properly if the dial indicator shows a change in elevation of less than 0.008 inch (0.20mm).

If the change is greater, then release all four clamping bars and repeat the securing process.

d. Loosen the four bolts to the base plate of the cam. Turn the handle to the left-right-hand threaded shaft to raise the cam and touch the aluminum plate of the beam. Manually rotate the cam 15-20 times to seat the total system. It may be necessary to raise the cam again so that it will always be in contact with the aluminum plate while it is rotating. If the lowest point of the cam does not touch the plate, then impact (knocking) will result when it is rotated rapidly. Now tighten the four bolts to the base plate of the cam.

e. Set the plate extensometer dial gauge which shows the deflection at a point one-half inch (12.5mm) to the left of the joint.

f. Zero both dial gauges and the revolution counter.

g. Energize the electric motor and record accumulative and repeated deflections of the beam and left plate at corresponding repetitions of deflection at increasing interval of time. Continue recordings to identify when a crack first appears and also when it goes through the beam.
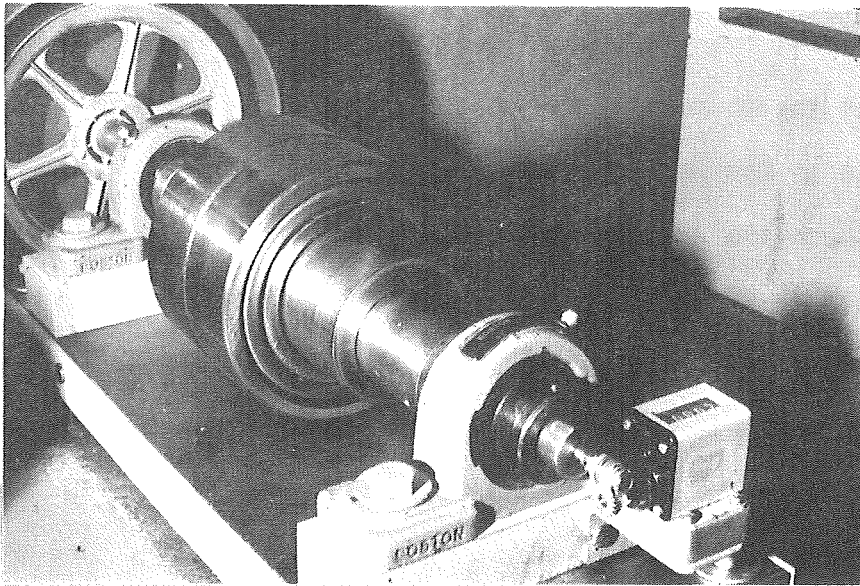
a. Variable Pitch Cam for Vertical Shear Test
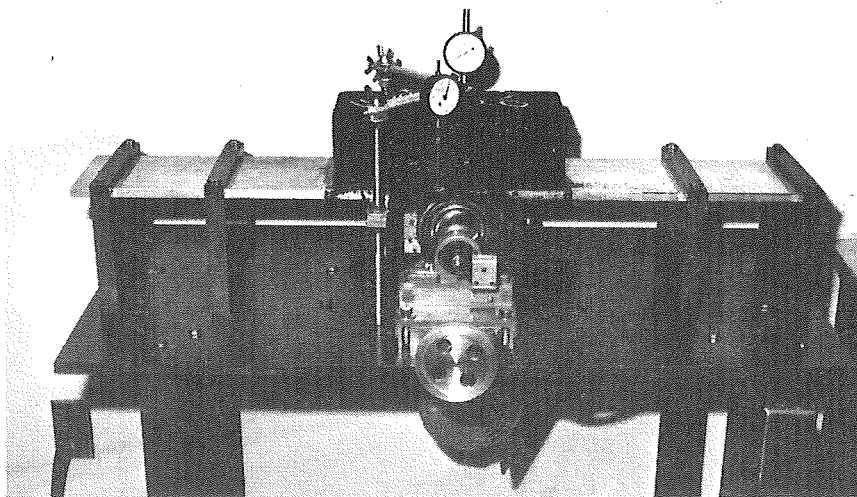
b. Asphaltic-Aluminum Beam in Vertical Shear Test Set-up

Figure 1F. Photographs of the Vertical Shear Test Equipment

BENDING OF A COMPOSITE BEAM

by

D. A. DaDeppo

Analysis

The system under consideration consists of two uniform beams
joined by a layer of deformable adhesive material of uniform thick-
ness. A short segment and a cross section of the composite beam
are shown in Figure 1G. The adhesive is capable of transmitting shear
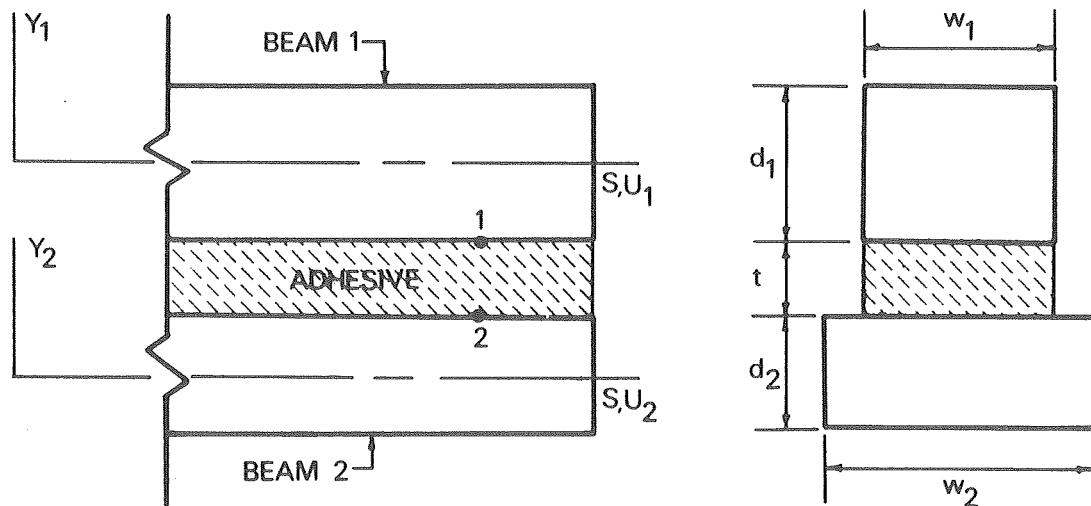stress as well as normal stress at points of bonding to the beams. It

Figure 1G. Composite Beam

is assumed that the normal stresses at points such as 1 and 2 (Figure 1G) are proportional to the change in thickness of the adhesive, e_t, and that the shear stresses are proportional to the axial component of the displacement of point 1 relative to point 2, e_a. The usual assumptions that plane cross sections of an undeformed beam remain plane and normal to the reference axis during bending are used in the analysis.

Let S be a common position coordinate measured along the centroidal axes of the beams. Let Y_1, U_1, and Y_2, U_2 be the transverse (deflection) and axial components of displacement of points at section S on the reference axes of beams 1 and 2, respectively. Then, for small strains and small rotations, the transverse and axial components of the displacement of point 1 with respect to point 2 (Figure 1G), respectively are

$$e_t = Y_1 - Y_2, \qquad (1)$$

$$e_a = \frac{d_1}{2} \frac{dY_1}{dS} + \frac{d_2}{2} \frac{dY_2}{dS} + U_1 - U_2. \qquad (2)$$

The resultant forces acting on beam elements of length dS are shown in Figure 2G. For equilibrium of each of the beam elements the forces must satisfy the differential equations of equilibrium:

$$\frac{dM_1}{dS} - V_1 - \frac{d_1}{2} F_a = 0, \qquad (3.1)$$

$$\frac{dV_1}{dS} + F_t = P_1, \qquad (4.1)$$

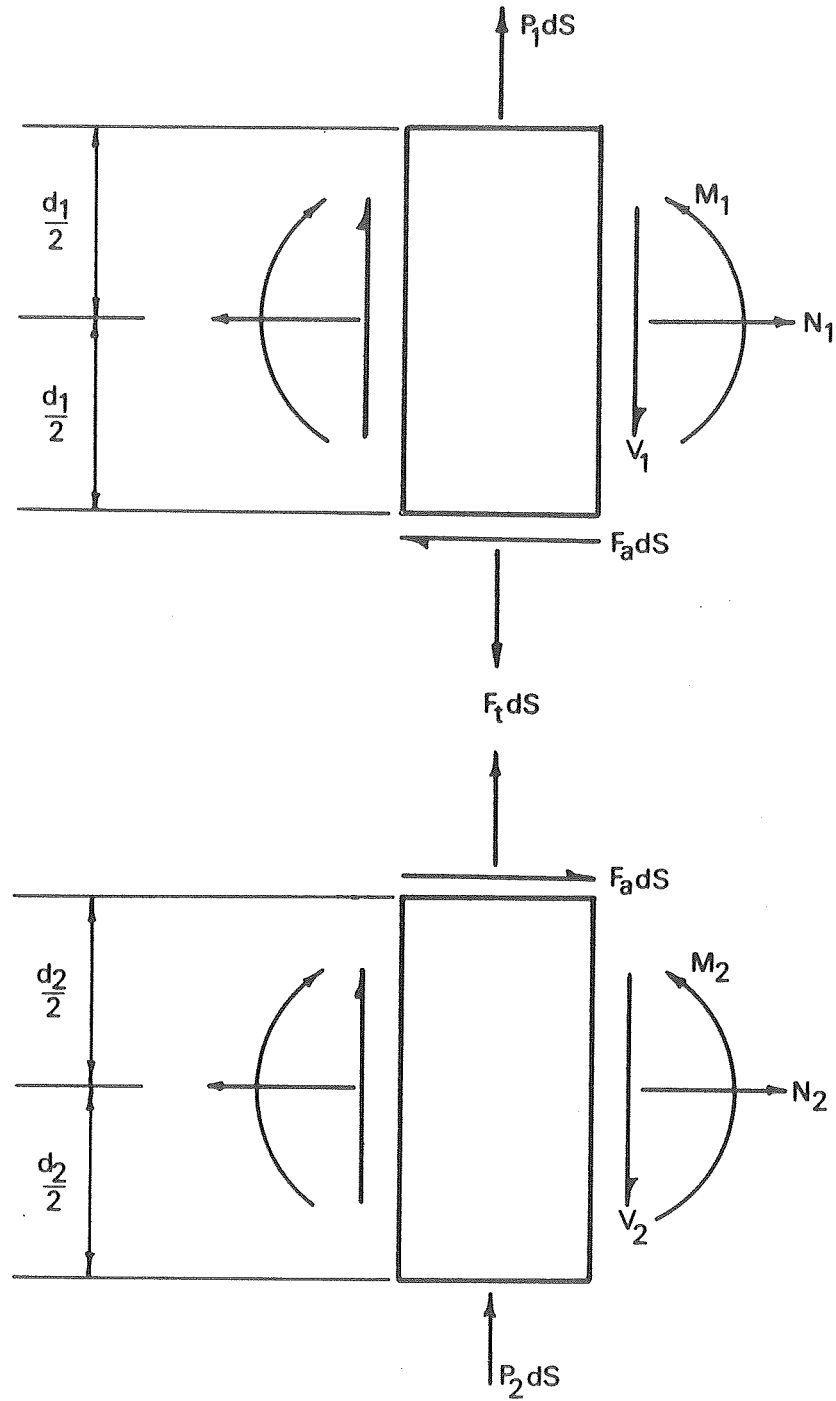$$\frac{dN_1}{dS} - F_a = 0, \qquad (5.1)$$

Figure 2G. Forces and Moments

$$\frac{dM_2}{dS} - V_2 - \frac{d_2}{2} F_a = 0, \tag{3.2}$$

$$\frac{dV_2}{dS} - F_t = P_2, \tag{4.2}$$

$$\frac{dN_2}{dS} + F_a = 0, \tag{5.2}$$

in which P_1 and P_2 are distributed transversely applied loads per unit of length and F_t and F_a are the normal and shear components of force per unit of length due to deformation of the adhesive.

It is assumed that the materials obey linear elastic stress-strain relations for which the integrated force-deformation relations become:

$$M_1 = E_1 I_1 \frac{d^2 Y_1}{dS^2}, \quad N_1 = E_1 A_1 \frac{dU_1}{dS} \tag{6.1 a,b}$$

$$M_2 = E_2 I_2 \frac{d^2 Y_2}{dS^2}, \quad N_2 = E_2 A_2 \frac{dU_2}{dS} \tag{6.2 a,b}$$

$$F_t = K_t e_t, \qquad F_a = K_a e_a \tag{6.3 a,b}$$

In equations (6), E_1 and E_2 are Young's moduli,

$$I_1 = W_1 d_1^3 / 12, \quad A_1 = W_1 d_1, \tag{6.4 a,b}$$

$$I_2 = W_2 d_2^3 / 12, \quad A_2 = W_2 d_2, \tag{6.5 a,b}$$

and K_t and K_a are tensile and shear moduli for the adhesive. Approximate values for these coefficients are given by

$$K_t = \frac{W_1 E_a}{t}, \quad K_a = \frac{W_1 E_a}{2(1+\nu_a)t} \tag{6.6 a,b}$$

in which E_a and ν_a are Young's modulus and Poisson's ratio for the adhesive.

Equations (1) through (6.3) may be combined to express the equations of equilibrium (3.1), (3.2), (5.1), and (5.2) in terms of displacements. The resulting governing equations are

$$E_1 I_1 \frac{d^4 Y_1}{dS^4} - \frac{K_a d_1}{2}\left(\frac{d_1}{2}\frac{d^2 Y_1}{dS^2} + \frac{d_2}{2}\frac{d^2 Y_2}{dS^2} + \frac{dU_1}{dS} - \frac{dU_2}{dS}\right) + K_t\left(Y_1 - Y_2\right) = P_1 \qquad (7)$$

$$E_2 I_2 \frac{d^4 Y_2}{dS^4} - \frac{K_a d_2}{2}\left(\frac{d_1}{2}\frac{d^2 Y_1}{dS^2} + \frac{d_2}{2}\frac{d^2 Y_2}{dS^2} + \frac{dU_1}{dS} - \frac{dU_2}{dS}\right) - K_t\left(Y_1 - Y_2\right) = P_2 \qquad (8)$$

$$E_1 A_1 \frac{d^2 U_1}{dS^2} - K_a\left(\frac{d_1}{2}\frac{dY_1}{dS} + \frac{d_2}{2}\frac{dY_2}{dS} + U_1 - U_2\right) = 0 \qquad (9)$$

$$E_2 A_2 \frac{d^2 U_2}{dS^2} + K_a\left(\frac{d_1}{2}\frac{dY_1}{dS} + \frac{d_2}{2}\frac{dY_2}{dS} + U_1 - U_2\right) = 0 \qquad (10)$$

It is convenient to employ nondimensional variables in constructing solutions of the equations. In the nondimensional equations:

$\bar{d} = d_1 + d_2$, $EI = E_1 I_1 + E_2 I_2$, l=characteristic length of beam

$S = ls$, $Y_1 = \bar{d} y_1$, $U_1 = \bar{d} u_1$, $Y_2 = \bar{d} y_2$, $U_2 = \bar{d} u_2$

$$\frac{d(\ )}{dS} = \frac{1}{l}\frac{d(\ )}{ds} \equiv \frac{1}{l}(\ )'$$

$E_1 I_1 = a_1 EI$, $E_2 I_2 = a_2 EI$, $d_1 = b_1 \bar{d}$, $d_2 = b_2 \bar{d}$, $\bar{d} = \rho l$

$M_1 = \dfrac{EI\bar{d}}{l^2} m_1$, $M_2 = \dfrac{EI\bar{d}}{l^2} m_2$, $V_1 = \dfrac{EI\bar{d}}{l^3} v_1$, $V_2 = \dfrac{EI\bar{d}}{l^3} v_2$

$N_1 = \dfrac{EI\bar{d}}{l^3} n_1$, $N_2 = \dfrac{EI\bar{d}}{l^3} n_2$, $P_1 = p_1 \dfrac{EI\bar{d}}{l^4}$, $P_2 = p_2 \dfrac{EI\bar{d}}{l^4}$

$K_t = \dfrac{EI}{l^4} \kappa_t$, $K_a = \dfrac{4EI}{\bar{d}^2 l^2} \kappa_a$

$\zeta_1 = \dfrac{12 a_1}{\rho^2 b_1{}^2}$, $\zeta_2 = \dfrac{12 a_2}{\rho^2 b_2{}^2}$.

From the defining equations one finds that

$a_1 + a_2 = 1$, $b_1 + b_2 = 1$.

The nondimensional bending moments, shears, and axial forces, expressed as derivatives of the nondimensional components of displacement are

$$m_1 = a_1 y_1'' \; , \tag{11.1}$$

$$v_1 = a_1 y_1''' - \kappa_a \left[b_1^2 y_1' + b_1 b_2 y_2' + \frac{2b_1(u_1 - u_2)}{\rho} \right] , \tag{12.1}$$

$$n_1 = \zeta_1 u_1' \; , \tag{13.1}$$

$$m_2 = a_2 y_2'' \; , \tag{11.2}$$

$$v_2 = a_2 y_2''' - \kappa_a \left[b_1 b_2 y_1' + b_2^2 y_2' + \frac{2b_2(u_1 - u_2)}{\rho} \right] , \tag{12.2}$$

$$n_2 = \zeta_2 u_2' \; , \tag{13.2}$$

and the governing equations (7) - (10) are

$$a_1 y_1'''' - \kappa_a \left[b_1^2 y_1'' + b_1 b_2 y_2'' + \frac{2b_1(u_1' - u_2')}{\rho} \right] + \kappa_t (y_1 y_2) = p_1 \tag{14.1}$$

$$a_2 y_2'''' - \kappa_a \left[b_1 b_2 y_1'' + b_2^2 y_2'' + \frac{2b_2(u_1' - u_2')}{\rho} \right] - \kappa_t (y_1 - y_2) = p_2 \tag{14.2}$$

$$\zeta_1 u_1'' - \kappa_a \left[\frac{2b_1 y_1'}{\rho} + \frac{2b_2 y_2'}{\rho} + \frac{4}{\rho^2}(u_1 - u_2) \right] = 0 \tag{14.3}$$

$$\zeta_2 u_2'' + \kappa_a \left[\frac{2b_1 y_1'}{\rho} + \frac{2b_2 y_2'}{\rho} + \frac{4}{\rho^2}(u_1 - u_2) \right] = 0 \tag{14.4}$$

Solution of the Governing Equations

The homogeneous equations corresponding to (14.1) - (14.4) have elementary solutions of the form

$$z_1 \equiv y_1 = C_1 e^{\lambda s}$$

$$z_2 \equiv y_2 = C_2 e^{\lambda s}$$

$$z_3 \equiv u_1 = C_3 e^{\lambda s} \tag{15}$$

$$z_4 \equiv u_4 = C_4 e^{\lambda s}$$

which may be written in matrix notation as $z = Ce^{\lambda s}$ where z and C are column vectors and the elements of C are constants. Substitution of (15) into (14) leads to a characteristic value problem for the determination of λ and C. The algebraic equations to be solved, written as a matrix equation, are

$$\begin{bmatrix} (a_1\lambda^4 - \kappa_a b_1^2\lambda^2 + \kappa_t) & (-\kappa_a b_1 b_2\lambda^2 - \kappa_t) & -2b_1\kappa_a\rho^{-1}\lambda & 2b_1\kappa_a\rho^{-1}\lambda \\ (-\kappa_a b_1 b_2\lambda^2 - \kappa_t) & (a_2\lambda^4 - \kappa_a b_2^2\lambda^2 + \kappa_t) & -2b_2\kappa_a\rho^{-1}\lambda & 2b_2\kappa_a\rho^{-1}\lambda \\ -2b_1\kappa_a\rho^{-1}\lambda & -2b_2\kappa_a\rho^{-1}\lambda & (\zeta_1\lambda^2 - 4\kappa_a\rho^{-2}) & 4\kappa_a\rho^{-2} \\ 2b_1\kappa_a\rho^{-1}\lambda & 2b_2\kappa_a\rho^{-1}\lambda & 4\kappa_a\rho^{-2} & (\zeta_2\lambda^2 - 4\kappa_a\rho^{-2}) \end{bmatrix} \begin{Bmatrix} c_1 \\ c_2 \\ c_3 \\ c_4 \end{Bmatrix} = 0 \quad (16a)$$

or,

$$A(\lambda)C = 0 \qquad (16b)$$

For nontrivial solutions of (16) we must have $A(\lambda) = 0$. Expansion of the determinant yields the characteristic equation

$$\lambda^6 - \frac{4\kappa_a}{3}\frac{(b_1^2 + b_2^2)}{a_1 \, a_2}\lambda^4 + \kappa_t\frac{\lambda^2}{a_1 a_2} - \kappa_a\kappa_t \frac{1 + \frac{1}{3}(b_1^2 + b_2^2)}{a_1 \, a_2} \quad \lambda^6 = 0 \qquad (17)$$

Equation (17) has $0 = \lambda_1 = \lambda_2 = \lambda_3 = \lambda_4 = \lambda_5 = \lambda_6$ as a six-fold repeated root. The factor which is cubic in $\lambda^2 = \mu$ has: 1. three real positive roots or, 2. one real positive root and two real negative roots or, 3. one real positive root and two complex conjugate roots. Attempts to further delimit the roots have not been successful. The main features of the analysis in all cases are adequately illustrated in the case of two complex conjugate roots. Thus, the remaining roots of equation 17 are taken in the form $\mu_1 = \lambda_7^2$, $\lambda_8^2 = (\pm d)^2$, $\mu_2 = \lambda_9^2$, $\lambda_{11}^2 = \{\pm(\alpha + i\beta)\}^2$, $\mu_3 = \lambda_{10}^2$, $\lambda_{12}^2 = \{\pm(\alpha - i\beta)\}^2$.

Elementary solutions corresponding to the six-fold repeated roots

are

$$z_1^T = \begin{bmatrix} 1, & 1, & 0, & 0 \end{bmatrix}, \tag{18.1}$$

$$z_2^T = \begin{bmatrix} 0, & 0, & 1, & 1 \end{bmatrix}, \tag{18.2}$$

$$z_3^T = \begin{bmatrix} s, & s, & 0, & \rho/2 \end{bmatrix}, \tag{18.3}$$

$$z_4^T = \begin{bmatrix} 0, & 0, & s, & s \end{bmatrix}, \tag{18.4}$$

$$z_5^T = \begin{bmatrix} s^2, & s^2, & 0, & \rho s \end{bmatrix}, \tag{18.5}$$

$$z_6^T = \begin{bmatrix} s^3, & s^3, & -\frac{3}{2}\rho\zeta_2\zeta^{-1}s^2, & (\frac{3}{2}\rho\zeta_1\zeta^{-1}s^2 + \frac{3}{4}\zeta_1\zeta_2\zeta^{-1}\kappa_a^{-1}\rho^3) \end{bmatrix}, \tag{18.6}$$

in which $\zeta = \zeta_1 + \zeta_2$

Elementary solutions corresponding to $\lambda_7 = a$ and $\lambda_8 = -a$ are

$$z_7^T = e^{as}\begin{bmatrix} C_{71}, & C_{72}, & C_{73}, & C_{74} \end{bmatrix} \equiv e^{as}C_7 \tag{18.7}$$

$$z_8^T = e^{-as}\begin{bmatrix} -C_{71}, & -C_{72}, & C_{73}, & C_{74} \end{bmatrix} \equiv e^{-as}C_8 \tag{18.8}$$

where C_{71}, C_{72}, C_{73}, C_{74} satisfy equations (16) when $\lambda = a$.

Complex elementary solutions corresponding to the roots $\lambda_9 = \alpha + i\beta$,

$\lambda_{10} = \alpha - i\beta$ $\lambda_{11} = -\alpha - i\beta$, $\lambda_{12} = -\alpha + i\beta$ are:

$$\bar{z}_9^T = e^{(\alpha+i\beta)s}\begin{bmatrix} C_{91}, & C_{92}, & C_{93}, & C_{94} \end{bmatrix} \equiv e^{(\alpha+i\beta)s}C_9^T,$$

$$\bar{z}_{10}^T = e^{(\alpha-i\beta)s}\begin{bmatrix} C_{91}^*, & C_{92}^*, & C_{93}^*, & C_{94}^* \end{bmatrix} \equiv e^{(\alpha-i\beta)s}C_9^{*T},$$

$$\bar{z}_{11}^{-T} = e^{(\alpha+i\beta)s}\begin{bmatrix} -C_{91}, & -C_{92}, & C_{93}, & C_{94} \end{bmatrix} \equiv e^{-(\alpha+i\beta)s}C_{11}^T,$$

$$\bar{z}_{11}^{-T} = e^{-(\alpha-i\beta)s}\begin{bmatrix} -C_{91}^*, & -C_{92}^*, & C_{93}^*, & C_{94}^* \end{bmatrix} \equiv e^{-(\alpha+i\beta)s}C_{11}^{*T},$$

in which $C_9^T = \begin{bmatrix} C_{91}, & C_{92}, & C_{93}, & C_{94} \end{bmatrix}$ satisfies equations (16) when

$\lambda = \alpha + i\beta$ and asterisks are used to denote conjugate quantities. Real

elementary solutions, which are preferred for numerical work, can be

derived by forming linear combinations of the complex solutions. Let

the vectors C_9 and C_{11} be expressed as

$$C_9 = a_9 + ib_9 \, , \quad C_{11} = a_{11} + ib_{11},$$

and let

$$f_1 = e^{\alpha s}\cos\beta s, \quad f_2 = e^{\alpha s}\sin\beta s \tag{18.9a, 10a}$$

$$f_3 = e^{-\alpha s}\cos\beta s, \quad f_4 = e^{-\alpha s}\sin\beta s, \tag{18.11a, 12a}$$

then

$$z_9 = f_1 a_9 - f_2 b_9, \tag{18.9}$$

$$z_{10} = f_2 a_9 + f_1 b_9, \tag{18.10}$$

$$z_{11} = f_3 a_{11} + f_4 b_{11}, \tag{18.11}$$

$$z_{12} = f_4 a_{11} - f_3 b_{11}, \tag{18.12}$$

are real elementary solutions corresponding to $\bar{z}_9$, $\bar{z}_{10}$, $\bar{z}_{11}$, $\bar{z}_{12}$.

The general solution of the homogeneous equations (14) is

$$z = \sum_{i=1}^{12} z_i(s)A_i \tag{19}$$

where the A_i are constants of integration. In the applications considered herein there are no distributed forces, i.e., $p_1 = p_2 = 0$. Therefore the complete solution is the general solution (19) of the homogeneous equations.

Derivatives of f_1, f_2, f_3, and f_4, which are needed for substitution in the boundary conditions and in the calculation of bending moments, shears, and axial force, are expressible as functions of f_1, f_2, f_3, f_4. Formulas for these derivatives are given below

$$f_1 = e^{\alpha s}\cos\beta s, \quad f_2 = e^{\alpha s}\sin\beta s,$$

$$f_1' = \alpha f_1 - \beta f_2, \quad f_1'' = (\alpha^2 - \beta^2)f_1 - 2\alpha\beta f_2, \quad f_1''' = (\alpha^3 - 3\alpha\beta^2)f_1 + (\beta^3 - 3\alpha^2\beta)f_2$$

$$f_2' = \alpha f_2 + \beta f_1, \quad f_2'' = (\alpha^2 - \beta^2)f_2 + 2\alpha\beta f_1, \quad f_2''' = (\alpha^3 - 3\alpha\beta^2)f_2 - (\beta^3 - 3\alpha^2\beta)f_1,$$

$$f_3 = e^{-\alpha s}\cos\beta s \;, \quad f_4 = e^{\alpha s}\sin\beta s,$$

$$f_3{}' = -\alpha f_3 - \beta f_4 \qquad f_3{}'' = (\alpha^2 - \beta^2)f_3 + 2\alpha\beta f_4, \quad f_3{}''' = -(\alpha^3 - 3\alpha\beta^2)f_3 + (\beta^3 - 3\alpha^2\beta)f_4,$$

$$f_4{}' = -\alpha f_4 + \beta f_3, \quad f_4{}'' = (\alpha^2 - \beta^2)f_4 - 2\alpha\beta f_3, \quad f_4{}''' = -(\alpha^3 - 3\alpha\beta^2)f_4 - (\beta^3 - 3\alpha^2\beta)f_3.$$

APPLICATION

The theory was applied to a composite beam as shown in Figure 3G. The purpose of the analysis was to determine how the thickness of the adhesive layer affects the shear and bending moment in Beam 1 at section 3. Because of the slot in Beam 2 at section 3 the governing equations must be solved separately for spans 23 and 2'3 and the 24 constants of integration must be chosen to satisfy boundary conditions at sections 2, 2', and 3. Overbars are used to identify coordinates, bending moment shear, and axial force for span 2'3; positive senses for these quantities are shown in Figure 3G. This choice of coordinates for span 2'3 permits direct, easy adaptation of the analytical developments to the problem. The boundary conditions for the problem are:

at $S=0$

$$0 = Y_2$$

$$0 = Y_2{}' - (\hat{a}l/3E_2 I_2)M_2$$

$$0 = U_2$$

$$0 = M_1$$

$$0 = V_1$$

$$0 = N_1$$

at $\overline{S}=0$

$$0 = \overline{Y}_2$$

$$0 = \overline{Y}_2{}' - (\hat{a}l/3E_2 I_2)\overline{M}_2$$

$$0 = \overline{N}_2$$

$$0 = \overline{M}_1$$

$$0 = \overline{V}_1$$

$$0 = \overline{N}_1$$

Figure 3G. Beams for Example Condition

$$\text{at } S = \bar{S} = 1$$

$$0 = M_2 \qquad\qquad 0 = Y_1 - \bar{Y}_1$$

$$-P = V_2 \qquad\qquad 0 = Y'_1 + \bar{Y}'_1$$

$$0 = N_2 \qquad\qquad 0 = U_1 + \bar{U}_1$$

$$0 = \bar{M}_2 \qquad\qquad 0 = M_1 - \bar{M}_1$$

$$0 = \bar{V}_2 \qquad\qquad 0 = V_1 + \bar{V}_1$$

$$0 = \bar{N}_2 \qquad\qquad 0 = N_1 - \bar{N}_1$$

The specific dimensions for the beam are

$\alpha = 0.5$, $1 = 12$ in.

$W_1 = 5$ in., $d_1 = 2$ in., $E_1 = 0.2 \times 10^6$ psi.

$W_2 = 6$ in., $d_2 = 0.5$ in., $E_2 = 10 \times 10^6$ psi.

$t = 0.375$ in., $E_a = 2 \times 10^3$ psi, $\nu_a = 0.45$

For the given dimensions and mechanical properties $E_1 I_1 / E_2 I_2 = 8/7.5$, which was taken to be unity in the calculations. Therefore, the nondimensional parameters are

$a_1 = a_2 = 0.5$, $b_1 = 0.8$, $b_2 = 0.2$, $\rho = 1/4.8$

$\kappa_a = 1.55$, $\kappa_t = 415$, $\zeta_1 = 216$, $\zeta_2 = 3456$, $\zeta = 3672$

with $\mu^2 = \lambda$, the cubic factor of equation (17) is

$\mu^3 - 2.8107\mu^2 + 1660\mu - 3739.43$

and, when set equal to zero has roots

$\mu_1 = 2.25437$, $\mu_2 = 0.27816 + 40.72675i$

$\mu_3 = 0.27816 - 40.72675i$

From these values we calculate

$$\lambda_7 = 1.50146, \quad \lambda_8 = -1.50146,$$

$$\lambda_9 = 4.52802 + 4.49720i = \alpha + i\beta,$$

$$\lambda_{10} = 4.52802 - 4.49720i,$$

$$\lambda_{11} = -4.52802 - 4.49720i,$$

$$\lambda_{12} = -4.52802 + 4.49720i,$$

and from equations (16) we obtain

$$C_7^T = \begin{bmatrix} 240.2072, & 239.3291, & -16, & 1 \end{bmatrix},$$

$$C_8^T = \begin{bmatrix} -240.2072, & -239.3291, & -16, & 1 \end{bmatrix},$$

and

$$C_9^T = \begin{bmatrix} (-1695.86 -1797.38i), & (1615.81 +1876.88i), & -16, & 1 \end{bmatrix}.$$

From the defining relations for a_9, b_9, a_{11}, and b_{11} we obtain

$$a_9^T = \begin{bmatrix} -1695.86, & 1615.81, & -16, & 1 \end{bmatrix}$$

$$b_9^T = \begin{bmatrix} -1797.38, & 1876.88, & 0, & 0 \end{bmatrix}$$

$$a_{11}^T = \begin{bmatrix} 1695.86, & -1615.81, & -16, & 1 \end{bmatrix}$$

$$b_{11}^T = \begin{bmatrix} 1797.38, & -1876.88, & 0, & 0 \end{bmatrix}$$

The details of the substitution of the solution functions into the boundary conditions are not presented here. The calculated values for the shear and bending moment at section 3 of beam 1 are

$$V_1(1) = 0.495P, \quad M_1(1) = -0.290Pl$$

For an adhesive layer of vanishing thickness, i.e., $t \to 0$

$$V_1(1) = 0.5P, \quad M_1(1) = -0.4Pl$$

Thus, we observe that the thickness of the adhesive layer has almost no effect on shear, but leads to a 25% reduction in the bending moment.